Food Bioscience 69 (2025) 106752



Contents lists available at ScienceDirect

Food Bioscience

journal homepage: www.elsevier.com/locate/fbio



# Hydrolysis of flavanones from orange peel and evaluation of anticancer potential using naringinase immobilized on corn cob powder

Kevin Esteban Garzón-Alonso [a], Maryli Jessenia Bohorquez-Peña [a], Brandon Vargas-Suaza [b], Julio Cesar Rendón-Londoño [c], Mónica Mesa [b], Yuly Nataly Franco-Tobón [d], Julián Paul Martínez-Galán [a,*]

[a] Laboratorio Alimentación y Nutrición Humana, Escuela de Nutrición y Dietética, Universidad de Antioquia, Carrera 75 # 65-87, Antioquia, Medellín, Colombia
[b] Grupo Ciencia de los Materiales CIENMATE, Facultad de Ciencias Exactas y Naturales, Universidad de Antioquia, Medellín, Colombia
[c] Facultad de Ciencias Básicas, Universidad Santiago de Cali, Cali, Colombia
[d] Facultad de Ciencias de la Nutrición y los Alimentos, Universidad CES, Medellín, Colombia

ARTICLE INFO

*Keywords:*
Naringinase
Flavanones
Orange
Corn cob
Enzyme immobilization

ABSTRACT

The management of waste from global orange production represents an environmental and economic challenge. In this study, the extraction of flavanones from orange peel albedo was optimized as a sustainable and economical alternative to purified substrates. The extracts obtained, rich in naringin, narirutin, hesperidin, neohesperidin and rutin, were enzymatically hydrolyzed by the naringinase complex, whose *α-L*-rhamnosidase and *β-D*-glucosidase activities transformed these compounds into prunin and naringenin. Their effect was evaluated in cell viability assays in the SW480 line, identifying compounds with potential biological activity in colon cancer prevention. Purification of naringinase increased its affinity for *α-L*-rhamnosidase activity, while its immobilization in corn cob powder allowed improving its reusability and stability, retaining up to 75 % of its initial activity after 10 consecutive cycles. By using whole extracts without purification, this study proposes a more viable and scalable approach for the valorization of citrus waste for biological purposes.

## 1. Introduction

World orange production reached 49.3 million metric tons (MMT) in 2020, with Brazil being the market leader with 16.9 MMT, followed by the United States with 4.11 MMT (Foreign Agricultural Service (FAS)., 2022) In the global context, Colombia ranks 28th, with a planted area of 528.543 ha in 2022. At the national level, oranges are the second most cultivated fruit, highlighting the Valencia orange variety (*Citrus sinensis [L.] Osbeck*) as the most cultivated in the department of Tolima, with 2.992 tons produced (Ministerio de Agricultura, 2024). However, beyond production, it is relevant to consider the management of by-products generated during fruit processing. In particular, in the production of orange juice, it is observed that approximately 50 % of the fresh weight of the fruit is converted into juice, while the remaining 50 % is composed of pulp, peel and seeds. Specifically, peels constitute 95 % of these residues, which underlines the importance of exploring strategies for their utilization or proper disposal (Ortiz et al., 2020; Rezzadori et al., 2012). These orange biocomposites are prioritized by the citrus sector in the department of Tolima, within the framework of the competitiveness pillar (Gobernación del Tolima, 2021).

Orange peel is composed of two main layers: the flavedo, which is the outer layer, and the albedo, the white inner layer; research has shown that the albedo contains a higher concentration of flavonoids compared to the flavedo (Ahmed et al., 2017; Y. C. Wang et al., 2008). Among the flavonoids present in albedo are hesperidin, rutin, and naringin, the latter is the most abundant flavanone in orange peel albedo, which has gained attention due to its biological properties, including activities, antioxidant, cardioprotective, antibacterial, antiviral, and

*Abbreviations:* EDA, Ethylenediamine; Rha-*p*NP, *p*-nitrophenyl-*α-L*-rhamnopyranoside; Glc-pNP, *p*-nitrophenyl-*β-D*-glucopyranoside; DPPH, 2,2-diphenyl-1-picrylhydrazyl; DNS, 3,5-dinitrosalicylic acid; BSA, Bovine Serum Albumin; SEM, Scanning Electron Microscope; DSC, Differential Scanning Calorimetry; TGA, Thermogravimetric Analysis; NgsaC IM, Immobilized Commercial Naringinase; NgsaP IM, Immobilized Purified Naringinase; N, Commercial Naringin; N*, Orange albedo extract; Na, Commercial Naringin hydrolyzed by NgsaC IM; Na*, Albedo extract hydrolyzed by NgsaC IM; aNa, Commercial Naringin hydrolyzed by NgsaP IM; aNa*, Albedo extract hydrolyzed by NgsaP IM.

* Corresponding author.
*E-mail address:* julian.martinez@udea.edu.co (J.P. Martínez-Galán).

https://doi.org/10.1016/j.fbio.2025.106752
Received 30 January 2025; Received in revised form 25 April 2025; Accepted 2 May 2025
Available online 7 May 2025
2212-4292/© 2025 The Authors. Published by Elsevier Ltd. This is an open access article under the CC BY-NC-ND license (http://creativecommons.org/licenses/by-nc-nd/4.0/).

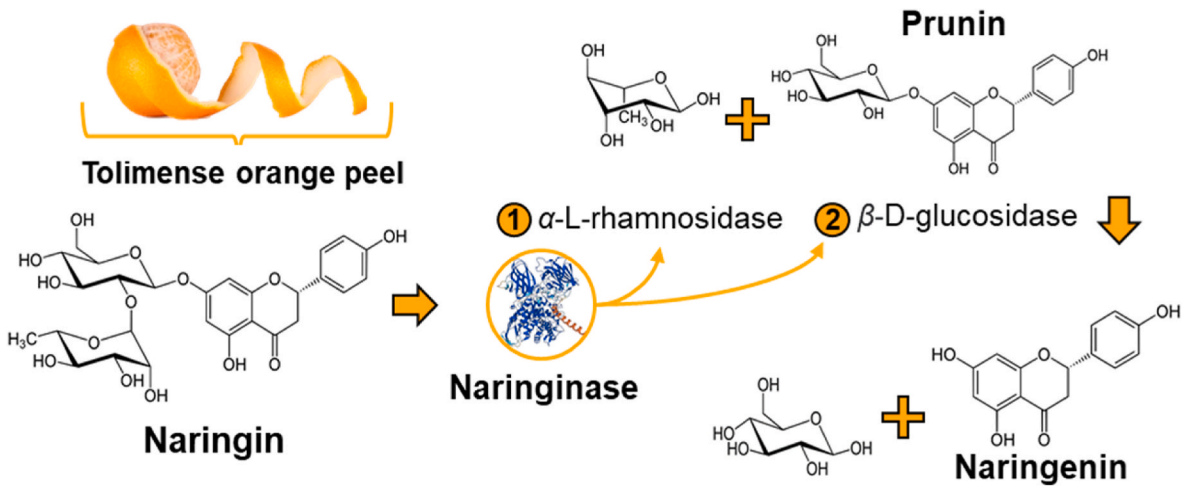



**Fig. 1.** Hydrolysis of naringin by naringinase (*α-L*-rhamnosidase and *β-D*-glucosidase). Source: Own elaboration.

anticarcinogenic (Ramesh et al., 2021; Shilpa, Farha, et al., 2023).

Naringinase is an enzyme complex that exhibits *α-L*-rhamnosidase and *β-D*-glucosidase activities, allowing the hydrolysis of various flavanones present in orange peel albedo. Prominent among these compounds are naringin, narirutin, hesperidin, neohesperidin and rutin, which can be converted into their respective aglycones of high antioxidant activity, such as naringenin and prunin, by enzymatic catalysis (Shilpa, Farha, et al., 2023). The mechanism of action of naringinase initiates with the activity of *α-L*-rhamnosidase, which releases rhamnose and prunin from flavanones present in the peel albedo. Subsequently, *β-D*-glucosidase acts on prunin, releasing glucose and generating naringenin as the final product (Fig. 1) (González et al., 2020).

The catalytic specificity of naringinase has been extensively investigated due to its potential for the biotransformation of flavonoid glycosides present in citrus by-products. Comparative studies employing natural and synthetic substrates reveal a clear substrate preference. For example, naringin exhibited the highest level of enzymatic hydrolysis, reaching up to 91 % conversion, significantly outperforming other structurally related compounds such as neohesperidin (16 %) and hesperidin (27 %) (Zhu et al., 2017). In support of these findings, kinetic data demonstrate a marked decrease in catalytic activity with increasing concentrations of less favorable substrates, while activity remains relatively high in the presence of naringin. Furthermore, substrate specificity assays indicate that naringin releases 33.0 nmol of rhamnose, a much larger amount compared to hesperidin (2.4 nmol) and rutin (8.2 nmol), with no detectable activity toward quercitrin. These results highlight the strong preference of the enzyme for α-1,2-rhamnosyl linkages, especially in naringin, and underline its applicability in the high-throughput production of bioactive aglycones such as naringenin and prunin from citrus residues (Manzanares et al., 1997; Yadav et al., 2013).

Since naringinase presents both catalytic activities, a partial purification process can be done to increase the selectivity of *α-L*-rhamnosidase, in order to evaluate prunin activity (Carceller et al., 2019). This flavonoid has been little investigated *in vitro* models, but it has been suggested that it might possess antiviral, anti-inflammatory, hypoglycemic and hypocholesterolemic activities (Chang et al., 2011). However, considering that naringinase is not adapted to function under extreme industrial conditions and the use of its free form hinders the recovery of the enzyme from the reaction medium, immobilized naringinase is necessary to obtain stable and easily recyclable preparations (Riseh et al., 2024).

In this context, enzyme immobilization emerges as a key strategy to optimize the use of enzymes such as naringinase in industrial applications. This process involves the attachment of enzymes to an inert support, which offers several advantages, such as the reuse of enzymes, the improvement of their stability, and the increase of their performance (Romero et al., 2014). Due to the variety of biocatalysts and the wide possibilities of their use after immobilization, there is no single optimal method of enzyme immobilization. In particular, covalent immobilization ensures strong and stable binding, which favors improved stability, efficiency, and multiple consecutive reuses. This, in turn, reduces long-term loss of activity and provides a specific environment that enhances selectivity in reactions (Bodakowska & Garncarek, 2022; Jackson et al., 2019).

The growing interest in producing biodegradable, low-cost, non-toxic and easily accessible materials from agro-industrial wastes, so in order to select a by-product that meets these conditions, four lignocellulosic wastes were evaluated by literature review: corn cob, sugarcane bagasse, wheat straw and rice husk. Corn cob stood out as the most favorable option due to its high cellulose content (45 %), a balanced proportion of hemicellulose (35 %) and low lignin content (15 %), which facilitates pretreatment and cellulose purification (Kenney et al., 2013; Khalid et al., 2017).

From an economic and environmental perspective, corn cob is obtained as an abundant and low-cost agricultural by-product, with a lower content of inorganic impurities (ash: 2.9 %), which makes it more efficient for the valorization of agroindustrial residues. Together, these factors position corn cob as the most suitable substrate for cellulose extraction in terms of purity, ease of processing, and sustainability (Kenney et al., 2013; Rocha-Meneses et al., 2017; Tayyab et al., 2018). In addition, corn is one of the most important crops worldwide, accounting for 39 % of global grain production. In the 2022/2023 season, global corn production was estimated at 1.2 billion tons, with the United States, China, and Brazil being the main producers (Gomes et al., 2024). However, the large amount of corn cobs remaining after harvest are often burned, contributing significantly to air pollution.

This study aimed to covalently immobilize naringinase, both in its commercial and purified form, using corn cob-derived cellulose as a support. Flavanones were produced from orange (*Citrus sinensis (L.) Osbeck*) peel albedo, with the purpose of obtaining a higher prunin content when using purified naringinase, and a mixture of naringenin and prunin when using commercial naringinase. The resulting compounds were evaluated for their biological potential, focusing on their effects on cell viability in SW480 colon cancer cells, a representative model of early-stage colorectal carcinoma. Flavanones, such as naringenin and prunin, have been shown to possess remarkable biological and anticancer potential through their ability to modulate various cell signaling pathways (Seong et al., 2023; Shilpa, Farha, et al., 2023). In particular, naringenin, the aglycone form of naringin, exhibits

anti-inflammatory, antioxidant, and antitumor properties, influencing gene expression and playing a crucial role in inhibiting uncontrolled cell proliferation and promoting apoptosis in cancer cells (Carceller et al., 2020; Ghanbari-Movahed et al., 2021; Wu et al., 2025).

## 2. Materials and methods

### 2.1. Materials

Commercial naringinase (Sigma-Aldrich) from *Penicillium decumbens*, naringin (Sigma-Aldrich), *p*-nitrophenyl-*α*-*L*-rhamnopyranoside (Rha-*p*NP), Sigma-Aldrich, *p*-nitrophenyl-*β*-D-glucopyranoside (Glc-*p*NP), D-Glucose monohydrate were used, corn cob powder obtained from local waste (Medellín-Colombia), ethylenediamine (EDA), sodium periodate, glutaraldehyde Sigma, cell line SW480 colon cancer lineage kindly donated by the Genética Regeneración y Cáncer (GRC) Universidad de Antioquia laboratory. The other reagents were analytical grade.

### 2.2. Orange peel extraction

#### 2.2.1. Material selection

Valencia oranges (*Citrus sinensis (L.) Osbeck*) were purchased from a commercial establishment in the city of Ibagué, Tolima-Colombia. Oranges that presented defects such as stains, bruises or visible deterioration were excluded. After selection, the oranges were washed, disinfected, and then the pulp was removed, separating the albedo from the peel. The initial moisture content of the albedo was determined gravimetrically through a vacuum drying process at 70 °C for 24 h (Chi et al., 2018).

#### 2.2.2. Statistical analysis: extraction of flavanones from orange peel albedo

Valencia' orange (*Citrus sinensis (L.) Osbeck*) albedo was crushed and divided into two fractions: one freeze-dried for 24 h and the other oven-dried at 55 °C for the same period. Subsequently, both materials were ground and subjected to extraction by maceration, based on Safdar et al. (2017) with modifications.

To optimize the extraction, a Central Composite Rotated Design (CCRD) with a $2^2$ factorial scheme, axial points and three replicates in the center, implemented in Statistica, StatSoft® (StatSoft Inc.), was used. Extractions were performed with a fixed sample/solvent ratio (1:10) and temperature of 50 °C, varying the extraction time and methanol concentration. All statistical analyses were performed at a significance level $\alpha = 0.05$ (95 % confidence), applying an ANOVA to evaluate linear, interaction and quadratic effects. The quality of the fit was quantified using the coefficient of determination ($R^2 = 98.30$ %) and the lack of fit analysis, the absence of significant discrepancies between the data and the model being considered acceptable.

The resulting extracts were filtered through Whatman No. 2 filter paper and centrifuged at 2795 *g* (RCF) for 10 min at room temperature (25 °C). The supernatant was collected and rotoevaporated at 40 °C and 19 (BUCHI Rotavapor, Flawil, Switzerland). Total flavanones (mg/mL) were then quantified using the modified Davis method (Kang et al., 2018; Kim et al., 2022).

#### 2.2.3. Determination of total flavanones

The amount of total flavanones (mg/mL) was quantified by the modified Davis (Kang et al., 2018; Kim et al., 2022). For quantification, aliquots of 100 μL of extract were mixed with 1000 μL of 90 % diethylene glycol and 100 μL of 1M NaOH, shaken vigorously and incubated at room temperature (25 °C) for 1 h before measuring their absorbance at 420 nm using a UV–VIS spectrophotometer (Thermo Scientific™, GENESYS™ 50). A naringin standard curve ($\varepsilon_{420nm} = 10.41$ $mM^{-1}$ $cm^{-1}$) was used.

#### 2.2.4. Estimation of the antioxidant capacity of extracts

Antioxidant activity was calculated using the DPPH reagent following the methodology described by (Rashid et al., 2022) with slight modifications. 100 μL of extract was mixed with a methanolic solution of DPPH (3.90 mL), subsequently incubated at room temperature (25 °C) under dark conditions for 30 min; antioxidant activity was assessed by measuring absorbance at 517 nm using a UV–VIS spectrophotometer (Thermo Scientific™, GENESYS™ 50). The amount of free radicals removed was calculated using Equation (1), where Ab sample represents the absorbance of the sample and Ab control the absorbance of the control (working solution and 80 % methanol).

$$\% \text{ Inhibition} = \left[ \left( Ab_{control} - Ab_{sample} \right) / Ab_{control} \right] \times 100 \qquad \text{Equation (1)}$$

### 2.3. Determination of naringinase enzymatic activity

For the determination of enzyme activity, the methodology described by (Carceller et al., 2019) was followed. The activities of *α*-*L*-rhamnosidase and *β*-*D*-glucosidase were determined by adding an aliquot of enzyme solution (50 μL) to 700 μL of 50 mM sodium citrate buffer (50 °C; pH 4.50) containing 50 μL of Rha-*p*NP (*p*-nitrophenyl-*α*-*L*-rhamnopyranoside) or Glc-*p*NP (*p*-nitrophenyl-*β*-*D*-glucoside) 0.5 mM. After 10 min of reaction, 800 μL of $Na_2CO_3$ (1 M) was added to stop the reaction, its absorbance was evaluated at 405 nm using a UV–VIS spectrometer (Thermo Scientific™ GENESYS™ 50 UV–Visible). A p-nitrophenol calibration curve ($\varepsilon_{405nm} = 4.74$ $mM^{-1}$ $cm^{-1}$).

#### 2.3.1. Measurement of enzyme activity by reducing sugars

Hydrolysis of naringin and reuse of the enzyme was performed using the method of (Miller, 1959) involving the combination of 250 μL of a 3, 5-dinitrosalicylic acid solution with 250 μL of sample, followed by heating at 100 °C for 5 min. After cooling, 2.50 mL of MilliQ water was added and absorbance was measured at a wavelength of $\lambda = 540$ nm. The concentration of released sugars was calculated using Lambert Beer's law and a molar extinction coefficient of ($\varepsilon_{540nm} = 100.54$ $mM^{-1}$ $cm^{-1}$), obtained from an analytical curve constructed using different glucose solutions in a range from 0 to 20 mm (Carceller et al., 2020).

### 2.4. Protein determination

Protein content on the naringinase complex was evaluated by the Bradford colorimetric method (Bradford, 1976). For the analysis, 0.1 mL of the enzyme sample was mixed with 1 mL of Bradford's reagent, the mixture was stirred at 250 rpm at 25 °C for 10 min. Subsequently, the optical density was determined at a wavelength of 595 nm using a UV–VIS spectrophotometer (Thermo Scientific™ GENESYS™ 50 UV–Visible). Protein quantification was performed based on a standard curve generated from bovine serum albumin (BSA; Sigma-Aldrich, USA) as a result of a absorptivity coefficient $\varepsilon_{595nm} = 2.54$ $(mg/mL)^{-1}$.

### 2.5. Purification of naringinase

Naringinase purification was performed following the methodology described by (Carceller et al., 2020). A dialyzed naringinase solution (50 mL of enzyme in Milli-Q water dialized for 24 h at 25 °C) was added to a DEAE-Sephacel chromatographic resin previously equilibrated with sodium phosphate buffer ($NaH_2PO_4/Na_2HPO_4$) 5 mM, (pH 6.80) and kept under agitation (200 rpm) for 1 h. The resin with the enzyme was separated from the solution by filtration and subsequently naringinase was desorbed using a NaCl gradient (50 mM, $V = 50$ mL). The enzyme solution obtained was analyzed using specific substrates as described in section 2.4.

### 2.6. Naringinase immobilization

#### 2.6.1. Pretreatment of corn cob

The corn cob delignification process was carried out following the methodology described by (Bassan et al., 2016). The corn cob was initially subjected to a grinding and sieving process (0.84 mm). It was then autoclaved compressed at 121 °C and 0.13 MPa using a 70 % ethanol solution with a 1:10 wt/volume ratio for 20 min, followed by rapid decompression. After autoclaving, an alkaline pretreatment of the corncob powder was performed by adding 2M NaOH at a ratio of 1:10, stirring the mixture for 24 h at room temperature (25 °C). It was filtered and the solid fraction of the treated biomass was washed twice with 500 mL of distilled water to remove residual NaOH until the pH was adjusted to a neutral value of the filtrates. Finally, after washing and filtration, the pretreated wet biomass was collected for further analysis and functionalization.

#### 2.6.2. Activation of aldehyde groups in corn cob cellulose

The activation of the aldehyde groups in the material was carried out following the methodology described by (Pietricola et al., 2020), with some modifications. To generate the aldehyde groups, the support was treated with $NaIO_4$ (100 mM), under constant stirring for 4 h at room temperature (25 °C). The amount of aldehyde groups generated was quantified by inverse ratio with $NaHCO_3$/KI. Aliquots of 100 μL of diluted samples were taken, to which 700 μL of $NaHCO_3$ solution and 700 μL of 10 % w/v KI solution were added, and the absorbance was measured at 450 nm using a UV–VIS spectrophotometer (C. Zhang et al., 2020) (Thermo Scientific™, GENESYS™ 50).

#### 2.6.3. Support functionalization

The functionalization of the material was based on the methodology described (Bassan et al., 2016). To carry out the amination of the support, 1 g of support was treated with $NaIO_4$ (100 mM) in a 1:15 w/v ratio, subjected to constant stirring for 4 h at room temperature (25 °C). The amount of aldehyde groups generated was quantified by reverse titration with $NaHCO_3$/KI and absorbance measurement at 450 nm before and after the oxidation process with $NaIO_4$, using a UV–VIS spectrophotometer (Thermo Scientific™, GENESYS™ 50 UV–Vis).

Chemical functionalization of the support continued with amination of the oxidized material. Ethylenediamine (EDA) 2 M (pH 10.0) was incorporated for 4 h in a 1:5 w/v mL ratio of EDA. Subsequently, $NaBH_4$ was added for 24 h to reduce the imines to amines. The support was washed with 0.1 M sodium acetate buffer (pH 4.0). To provide the aldehyde groups that allow covalent immobilization with the amino groups of the enzyme, glutaraldehyde in 200 mM phosphate buffer (pH 7.0) was used, incorporating 6 mL of 15 % glutaraldehyde per 1 g of wet material at 250 rpm at room temperature (25 °C) for 15 h. The excess glutaraldehyde was washed with water and then with 25 mM sodium phosphate buffer (pH 7.0).

#### 2.6.4. Enzyme immobilization

After functionalization of the support, enzyme immobilization was performed following the methodology of (Carceller et al., 2020), for each gram of activated support, 10 mL of 5 mM/L sodium phosphate buffer (pH 7.0) containing an enzyme load of 1 mg protein/g support was added. The suspension was subjected to agitation (250 rpm) for 90 min at 25 °C. $NaBH_4$ was then added for 1 h to reduce the imines to amines and form covalent immobilization.

The enzymatic activity of the supernatant, the immobilized material and the residual protein were determined during the immobilization process (Bradford, 1976) and expressed as relative enzyme activity yield (0–100 %) and relative protein (0–100 %). Finally, the immobilization yield was evaluated (Equation (2)).

$$\text{Immobilization yield } (\%) = [(X_1 - X_2) / X_1] \times 100 \qquad \text{Equation (2)}$$

where $X_1$ is the offered protein concentration for immobilization and $X_2$ is the protein concentration present in the supernatant after immobilization.

### 2.7. Physicochemical and biochemical characterization of immobilized naringinase

#### 2.7.1. Scanning electron microscope (SEM)

Scanning Electron Microscopy (SEM) was performed to observe the morphology of both delignified and undelignified corn cobs, with the objective of analyzing the influence of morphology on catalytic processes. A JEOL-JSM 6490LV scanning electron microscope (JEOL Ltd., Tokyo, Japan) with an operating voltage of 20 kV and magnifications of 3000× and 500 × was used. The samples, in the form of thin squares, were fixed on graphite and coated with gold prior to analysis (Méndez et al., 2022).

#### 2.7.2. Characterization using Fourier transform infrared spectroscopy (FT-IR)

Each step of the methodology was characterized using Fourier transform infrared spectroscopy (FT-IR). A PerkinElmer Spectrum Two FT-IR spectrophotometer equipped with a Smart Orbit diamond attenuated total reflection (ATR) attachment was used. Absorption spectra were acquired in the 4000-500 $cm^{-1}$ range, averaging 16 scans, with a resolution of 4 $cm^{-1}$ (Méndez et al., 2022).

#### 2.7.3. Differential Scanning Calorimetry (DSC)

The glass transition temperatures of untreated, delignified, oxidized and immobilized corn cob were determined by Differential Scanning Calorimetry (DSC) on Q100TA Instruments analyzer, weighing approximately 8 mg. The samples were weighed into aluminum containers, which were accurately weighed and sealed. The capsules were positioned in the calorimeter and the temperature was raised from 0 to 200 °C at a rate of 10 °C/min, while using an empty container as a reference (Méndez et al., 2022).

#### 2.7.4. Thermogravimetric analysis (TGA)

The thermal stability and thermal degradation behavior of corn cob, delignified corn cob, oxidized corn cob, immobilized corn cob (NgsaC IM and NgsaP IM) was characterized by thermogravimetric analysis (TGA). Sample weight loss measurements were carried out using a TA instrument, model Q500. Samples of approximately similar weight, 10 ± 1 mg, were used in a nitrogen atmosphere and heated to 600 °C at a heating rate of 10 °C/min (Méndez et al., 2022).

#### 2.7.5. Determination of Michaelis-Menten constant and maximum velocity ($K_M$)

The kinetic parameters of the enzyme (commercial and pure), both in free and immobilized form, were determined by measuring the reaction rates under the conditions mentioned in the numeral of section 2.4 using with substrate concentrations of Rha-*p*NP and Glu-*p*NP between 6.00 × $10^{-3}$ and 0.31 mM and a reaction time constant of 10 min. Michaelis Menten constants and maximum velocity ($K_M$ y $V_{max}$) were determined from Lineweaver-Burk plots (Carceller et al., 2019).

#### 2.7.6. Determination of catalytic activity as a function of pH and temperature

The effect of pH on the catalytic activity of the commercial and purified enzyme in its free and immobilized forms was evaluated by incubation in the presence of the specific substrate Rha-*p*NP and Glc-*p*NP under universal Mcllvaine buffer with pH varying from 2.00 to 7.00. The activity measurements were performed at different pH values of incubation, following the same experimental conditions mentioned in section 2.4, addition, the optimum temperature for hydrolysis of Rha-*p*NP and Glc-*p*NP was determined by measuring the enzyme activity (commercial and purified) in free and immobilized forms at temperatures

between 25 and 90 °C, under the same experimental conditions described previously (Carceller et al., 2020).

#### 2.7.7. Determination of catalytic activity and reuse of immobilized enzymes using naringin as a substrate

It was evaluated by weighing 80 mg of immobilized naringinase and 8.60 mM naringin extract obtained from orange peel as substrate, in universal McIlvaine buffer (50 mM at pH 4.50) at 70 °C for 60 min. After the reaction, the mixture was centrifuged at 4024.8 *g* (RCF) for 5 min at room temperature (25 °C) to remove the enzyme derivative, followed by three washes with 50 mM universal McIlvaine buffer (pH 4.50) before being used in a subsequent reaction cycle performing up to 10 reuses.

#### 2.7.8. Storing stability of immobilized and purified commercial naringinase

The stability of the activity of immobilized commercial naringinase (NgseC IM) and immobilized purified naringinase (NgseP IM) during prolonged periods of storage was determined by analyzing their activity at the time of immobilization (week 0) and subsequently at 2, 4, 6 and 8 weeks of storage at 4 °C. The evaluation of the activity of the immobilized enzymes was performed using the DNS method explained in section 2.7.6.

### 2.8. In vitro evaluation of flavanones biological activity

This study examined the direct impact of different treatments of flavanones extracted from orange peel albedo, along with their hydrolysates on the SW480 colon adenocarcinoma cell model. The treatments included commercial naringin (N), naringin hydrolyzed with immobilized naringinase (Na), naringin hydrolyzed with purified naringinase (aNa) and flavanones extracted from orange peel (N*). Additionally, flavones treated with commercial immobilized enzyme (Na*) and purified immobilized enzyme (aNa*) were also evaluated.

#### 2.8.1. Cell lines and culture medium

The effect on cell viability was assessed using the sulforhodamine B colorimetric method. SW480 cells were seeded at 15,000 cells per well in 96-well plates in DMEM media, supplemented with 3 % horse serum, cells were maintained at 37 °C and 5 % $CO_2$ in medium. 24 h after seeded, the culture medium was replaced and supplemented with the corresponding treatments, and their effects were evaluated at 24 and 48 h post-treatment.

After the exposure time, the cell monolayers were fixed with 10 % (w/v) trichloroacetic acid for 1 h at 4 °C and subsequently stained with $5.7 \times 10^{-2}$ % (w/v) sulforhodamine B solution for 30 min. The stain excess was removed by multiple washes with 1 % (v/v) acetic acid. The plates were incubated with 10 mM Tris solution (pH 10.50) at 55 rpm. Finally, the absorbance, which reflects the amount of viable cells, was measured using an EnSpire® microplate reader (PerkinElmer, USA) at a wavelength of 510 nm (Ferreira et al., 2013).

#### 2.8.2. Cell viability test

The effect on cell viability was assessed using the sulforhodamine B colorimetric method. SW480 cells were seeded in 96-well plates and incubated for 24 h at 37 °C and 5 % $CO_2$. The corresponding treatments were applied, using assay-specific cell densities 15,000 cells/well for the cell viability assay. At the time of treatment, cell monolayers were fixed with 10 % (w/vol) trichloroacetic acid for 1 h at 4 °C and stained with $5.7 \times 10^{-2}$ % (w/vol) sulforhodamine B solution in each well for 30 min, then washed with 1 % (vol/vol) acetic acid and allowed to dry overnight; finally, they were incubated with 10 mM Tris solution (pH 10.50) at 55 rpm. Cell density was calculated using the EnSpire® microplate reader (PerkinElmer, USA) at a wavelength of 510 nm (Ferreira et al., 2013; Londoño et al., 2023).

**Table 1**
Central composite rotational design matrix (CCRD) composed of 2 replicates for flavanone extraction using the modified Davis method (Kang et al., 2018; Kim et al., 2022).

| | Coding | | Variables | | Drying | Freeze-drying |
|---|---|---|---|---|---|---|
| N° | $X_1$ | $X_2$ | A | B | mg/g | mg/g |
| 1 | −1 | −1 | 60.0 | 10 | 2.12 ± 0.01 | 2.62 ± 0.01 |
| 2 | 1 | −1 | 90.0 | 10 | 2.10 ± 0.01 | 2.56 ± 0.01 |
| 3 | −1 | 1 | 60.0 | 50 | 4.40 ± 0.01 | 4.80 ± 0.02 |
| 4 | 1 | 1 | 90.0 | 50 | 3.89 ± 0.03 | 4.29 ± 0.01 |
| 5 | 1.41 | 0 | 96.0 | 30 | 2.92 ± 0.01 | 3.32 ± 0.02 |
| 6 | −1.41 | 0 | 54.0 | 30 | 3.51 ± 0.01 | 3.95 ± 0.01 |
| 7 | 0 | 1.41 | 75.0 | 58.2 | 4.82 ± 0.01 | 5.46 ± 0.01 |
| 8 | 0 | −1.41 | 75.0 | 1,8 | 1.48 ± 0.01 | 1.58 ± 0.02 |
| 9 | 0 | 0 | 75.0 | 30 | 4.83 ± 0.01 | 5.45 ± 0.02 |
| 10 | 0 | 0 | 75.0 | 30 | 4.98 ± 0.02 | 5.49 ± 0.02 |
| 11 | 0 | 0 | 75.0 | 30 | 4.71 ± 0.01 | 5.47 ± 0.02 |

## 3. Results and discussion

### 3.1. Flavanone extraction

Flavanones extracted from citrus fruits possess beneficial properties such as antioxidant, anticancer, antiviral and anti-inflammatory activity. However, their high moisture content (70–80 %) makes them susceptible to degradation. To counteract this, the methods described in (2.3.2.) were applied and variables were optimized using a central composite design (CCD). Extraction time and methanol concentration were evaluated in Table 1.

#### 3.1.1. Comparison of flavanone yields: dried samples vs. Lyophilized

The freeze-drying method showed a higher yield of flavanones compared to conventional drying. Fig. 2 presents the experimental matrix and the results obtained. Both methods achieved good flavanone extraction. Both conventionally dried peel samples and those subjected to freeze-drying showed satisfactory flavanone extraction performance. This result is supported by previous studies that have explored various non-conventional extraction techniques, such as ultrasound and other innovative methodologies (Martín et al., 2022; Tobón, 2020; Hasni et al., 2021), obtaining comparable results. This set of findings positions the extraction method by maceration and polar solvents as an efficient and reliable extraction method for obtaining flavanones.

The analysis of variance (ANOVA) indicated that, in both extraction methods evaluated (conventional drying and freeze-drying), the extraction time (B) was the most statistically significant variable ($p < 0.05$), followed by the quadratic effects AA and BB. The fitted model for the conventional drying method showed a coefficient of determination ($R^2$) of 99.35 % and a coefficient of variation (CV) of 4.2 %, while the freeze-drying method yielded an $R^2$ of 98.20 % and a CV of 5.8 %, demonstrating high predictive capability and adequate experimental precision in both cases. Additionally, the lack-of-fit test was not significant ($p = 0.12$ and $p = 0.08$, respectively), confirming the suitability of the model for the experimental data. According to the established criteria ($R^2 \geq 0.90$; CV $\leq$ 10 %), both models were considered statistically acceptable. Process optimization revealed that a methanol concentration close to 73 % and an extraction time of approximately 43 min led to optimal yields of 5.211 mg/mL for conventionally dried samples and 5.838 mg/mL for freeze-dried samples. Experimental validation showed minimal variation between predicted and observed values, with standard errors and deviations within acceptable limits, confirming good repeatability of the proposed extraction procedure.

The present study corroborates previous studies by Pereira et al. (2017), who found that more polar solvents such as methanol are more effective in the extraction of flavanone glycosides, such as naringin and hesperidin. Also, our results agree with studies conducted by Haida et al. (2022); Sawalha et al. (2009), who employed the maceration method

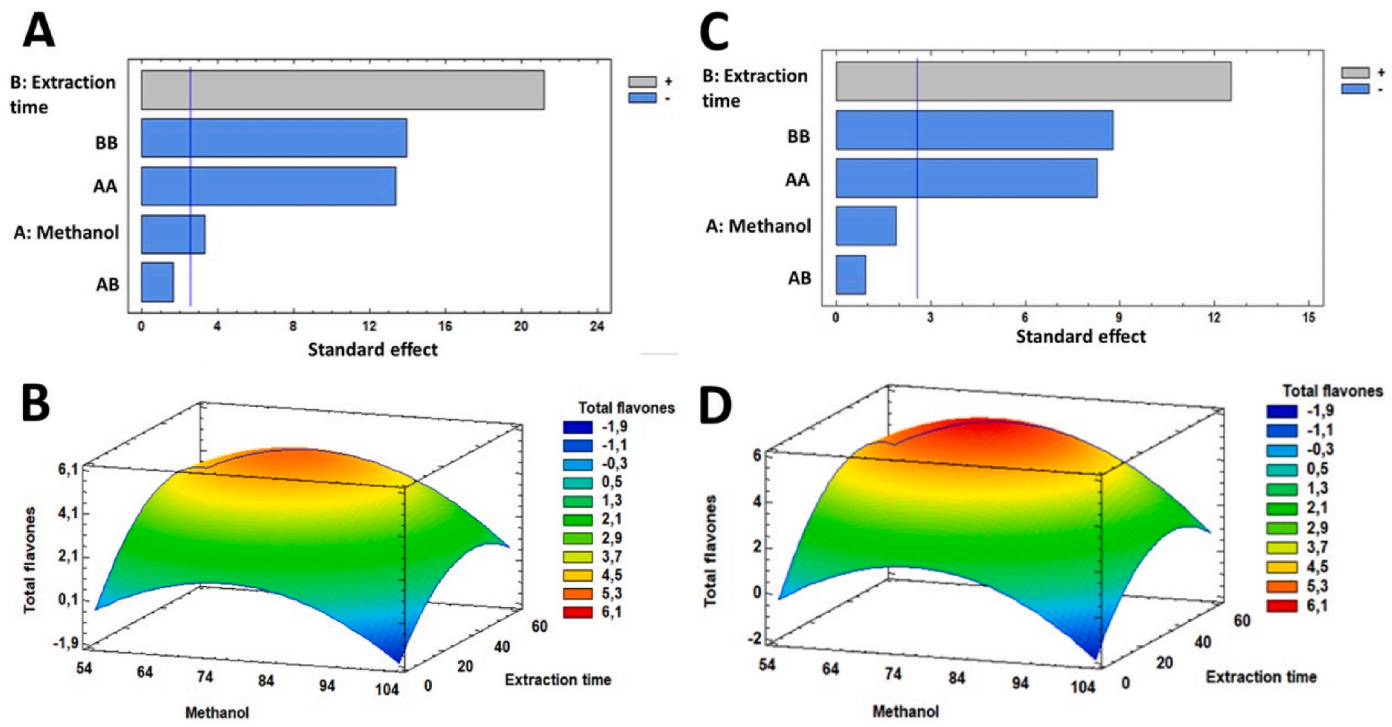



**Fig. 2.** Pareto diagram of drying method (A); response surface analysis of drying method (B); Pareto diagram of freeze-drying method (C); response surface analysis of freeze-drying method (D).

**Table 2**
Rhamnosidase and glucosidase activities of commercial naringinase (Ngsa C) and purified naringinase (Ngsa P). All values are expressed as mean ± standard deviation ($n = 3$).

| Purification | Protein (mg/mL) | Rha (U/mg) | Glu (U/mg) | Rha/Glu |
|---|---|---|---|---|
| Commercial | 0.50 ± 0.01 | 16322.60 ± 2.53 | 12530.90 ± 8.32 | 1.30 ± 6.63 × $10^{-4}$ |
| Dialysis | 0.43 ± 0.07 | 17461.40 ± 4.32 | 13063.50 ± 7.23 | 1.34 ± 4.09 × $10^{-4}$ |
| Purified | 0.12 ± 0.02 | 6800.80 ± 4.32 | 562.60 ± 3. 93 | 12.09 ± 7.68 × $10^{-2}$ |

Note: Rha/Glu values were calculated from measured enzymatic activities.

and obtained comparable results in the quantification of flavanones in orange peels. These comparisons support the validity of flavanone extraction in the present study and suggest a solid basis for the optimization of the extraction performed.

### 3.2. Naringinase purification

Table 2 shows that both commercial and dialyzed naringinase exhibit comparable levels of enzyme activity. However, the purified enzyme exhibits a marked increase in selectivity toward $\alpha$-L-rhamnosidase activity, which is reflected in the significant decrease in β-D-glucosidase activity. This change is quantified through the Rha/Glu activity ratio, an indicator of enzyme specificity defined as the ratio of $\alpha$-L-rhamnosidase activity (Rha) to $\beta$-D-glucosidase activity (Glu).

In commercial naringinase, this ratio is 1.30, whereas in the dialyzed enzyme it increases slightly to 1.34. However, after purification, the Rha/Glu ratio increases dramatically to 12.09, which is equivalent to a

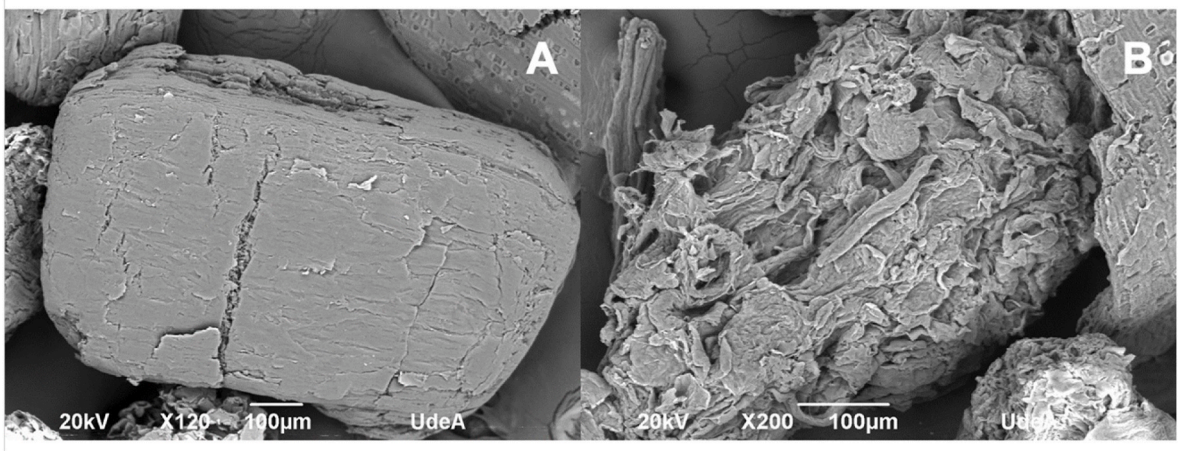



**Fig. 3.** Scanning electron microscopy (SEM) of corn cob powder before and after physicochemical pretreatment: (a) unmodified corn cob, (b) delignified material.

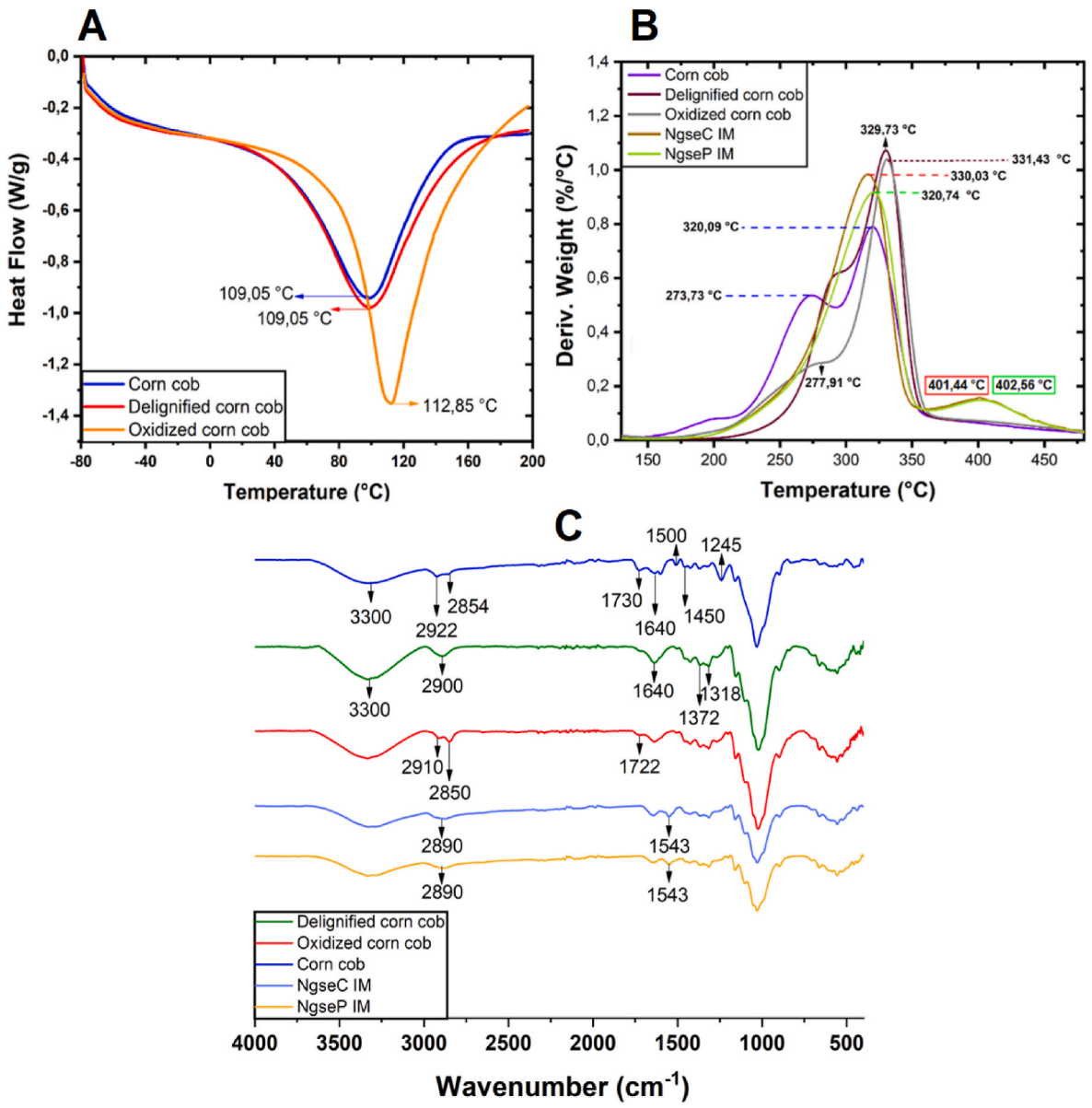



**Fig. 4.** Differential Scanning Calorimetry DSC (A) of corn cob (blue), delignified (red), oxidized (yellow); Thermogravimetric TGA analysis (B) of corn cob (blue), delignified (black), oxidized (gray), immobilized commercial naringinase (orange), immobilized purified naringinase (yellow); FT-IR spectra of corn cob (dark blue), delignified corn cob (green), oxidized (red), immobilized commercial naringinase (light blue), immobilized purified naringinase (yellow).

more than 9-fold increase in the enzyme's preference for hydrolysis of *α-L*-rhamnosidic bonds compared to *β*-D-glucosidic bonds. This is in agreement with the higher prunin content reported previously under the same purification conditions mentioned in section 2.6 in the methodology (Karamitros et al., 2024).

The significant increase in the selectivity of *α-L*-rhamnosidase after purification not only highlights the effectiveness of the process by a simple and practical method, but also underlines its relevance in the selective production of prunin (Li et al., 2021). Prunin is a bioactive compound with important therapeutic and pharmacological properties, making it valuable for various industrial applications (Borzova, 2023; Shilpa, Shams, et al., 2023). By increasing the selectivity of the enzyme towards prunin, the efficiency of the process is improved, allowing this compound to be obtained in larger quantities and with fewer unwanted by-products (Fang et al., 2019; Kapešová et al., 2019). This not only has economic implications, by reducing purification costs, but also opens the door to new research on its potential in areas such as biotechnology, pharmaceuticals and nutraceuticals production.

### 3.2.1. *Characterization of the delignification process*

The analysis of the morphology of treated and untreated corn cob by SEM (Fig. 3A–B) showed that decompression and NaOH treatment produced a significant decrease observed in Fig. 3B, which led to elimination of the surface layer and increased irregular structures with evident fissures along its extension (Fig. 3B) (Maceda et al., 2021; Waghmare et al., 2022). This increase in the rugose structure could offer a larger surface area, with higher amount of reactive functional groups, favoring functionalization and immobilization processes.

FT-IR spectra evidenced modifications in the functional groups of corn stover fibers before and after pretreatment (Fig. 4C), reflecting changes in the chemical structure of lignin and hemicellulose. In particular, the disappearance of the peak at 1730 $cm^{-1}$, associated with the stretching of the carbonyl bond (-C=O) of the ester bond in hemicellulose, was observed, confirming the success of the delignification process. Likewise, peaks in the 2922-2854 $cm^{-1}$ region, corresponding to the symmetric and asymmetric CH and $CH_2$ stretches in cellulose (guaiacol and syringyl) characteristic of angiosperms, showed a

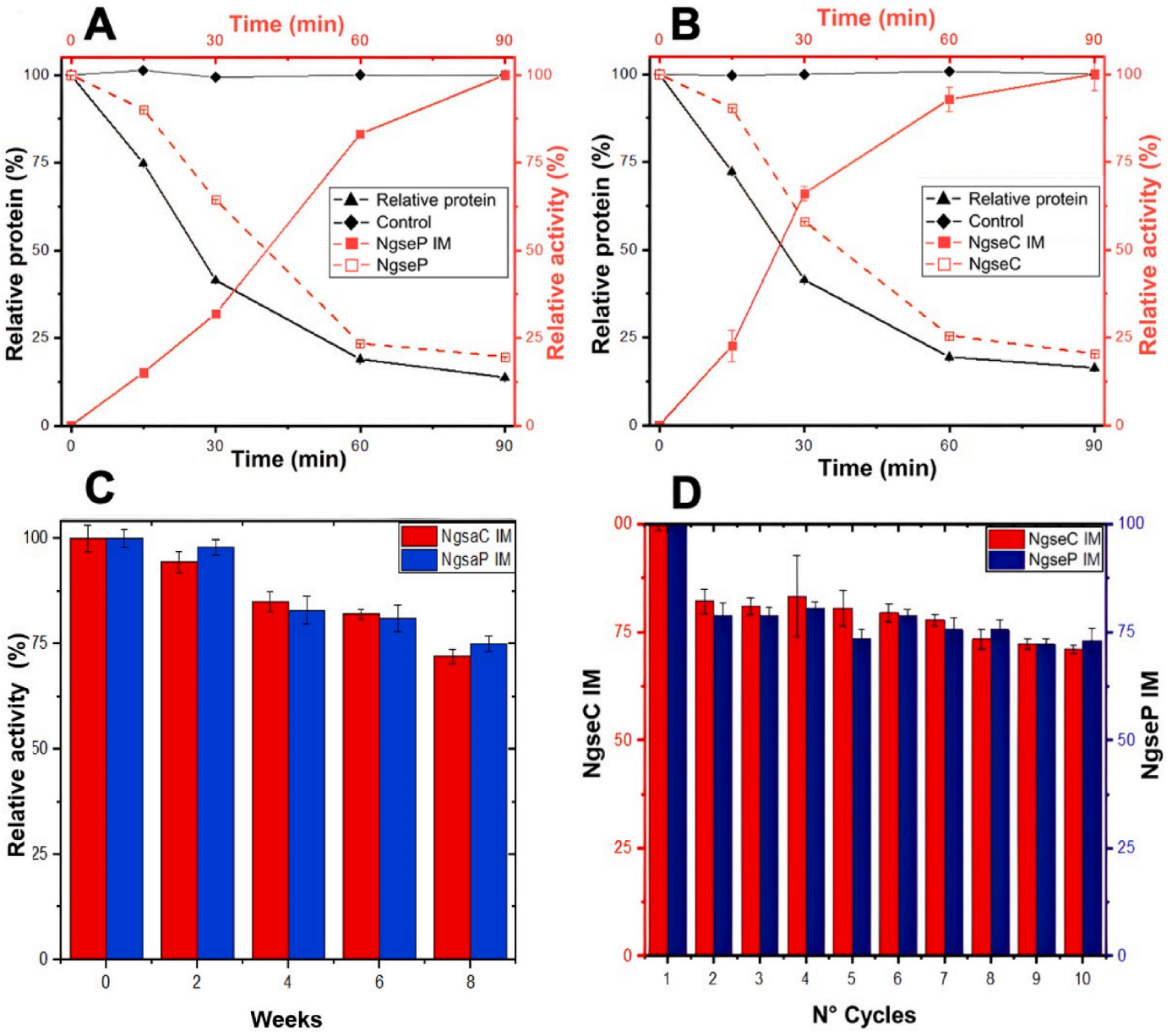



**Fig. 5.** Efficiency of Enzyme immobilization process: Immobilized Purified Naringinase "Ngsa P IM" (A); Immobilized Commercial naringinase "NgsaC IM" (B); Stability over weeks through reuse of NgsaC enzymes of NgsaC IM and NgsaP IM (C) and catalytic cycles of NgsaC IM and NgsaP IM (D).

decrease after pretreatment, suggesting a reduction in the amount of lignocellulose present in the material (Agustín Maceda et al., 2021; da Silva et al., 2013; Joelmy Zara et al., 2017).

On the other hand, a higher intensity was observed in the 3330 $cm^{-1}$ band, attributed to the stretching of O-H groups, indicating the breaking of hydrogen bonds in cellulose (Kumar & Pandey, 2013). In addition, the peak at 1640 $cm^{-1}$, associated with the bending vibration of the -OH groups, suggests the presence of adsorbed water in the structure of the material (Joelmy Zara et al., 2017). The decrease in peak intensity between 1500 and 1450 $cm^{-1}$ in the pretreatment spectra indicates a partial removal of lignin. Finally, the intensity changes in the 1330-1372 $cm^{-1}$ band, attributable to OH deformation of phenolic compounds and CH bending at -C-$CH_3$, confirm the partial removal of lignin in the treated material (Bassan et al., 2016).

Thermal transitions during corn cob delignification were studied by DSC (Fig. 4A). It was analyzed that the melting temperature of untreated corn cob powder was 99.46 °C, attributed to the presence of amorphous components such as hemicellulose and lignin, which contribute to moisture retention. On the other hand, delignified samples presented lower amounts of these compounds, showing slightly lower melting points (97.29 °C) (Veeramachineni et al., 2016).

The TGA analysis showed that the chemical composition of the material changed after delignification (Fig. 4B). Between 30 and 120 °C an initial mass loss of 2.10 % for the untreated material and 2 % for the delignified one was observed, which was due to low molecular weight compounds and volatile compounds (Valdés et al., 2015). An additional 27.90 % weight loss was lost at the maximum temperature of 273.73 °C due to hemicellulose processing, this loss can be attributed to the loss of xylan, arabinoxy, acetyl, wax and nitrogen containing compounds (Morán et al., 2008).

The intrinsic composition of lignocellulosic biomass contains three main components: cellulose, hemicellulose and lignin. Hemicellulose has an amorphous structure and is easily extracted during delignification, especially when NaOH is used (Abraham et al., 2020). This compound can remove lignin while extracting hemicellulose (Rocha et al., 2014). The NaOH solution affects and destroys the structure of the

crystalline and amorphous parts of lignin, allowing part of the hemicellulose to separate, the OH ions of NaOH break the bonds in the main lignin chain, while $Na^+$ ions combine with the lignin to form sodium phenate (Permata et al., 2021).

Previous studies observed losses similar to those found in this study in delignified cellulose, which is due to the intrinsic composition of lignocellulosic biomass, which includes cellulose, hemicellulose and lignin. Hemicellulose, with its amorphous structure, is easily extracted during delignification, especially with NaOH, which can remove lignin and extract hemicellulose simultaneously. NaOH destroys the crystalline and amorphous parts of lignin, allowing some of the hemicellulose to separate; the OH ions in NaOH break the bonds in the main lignin chain, while $Na^+$ ions combine with the lignin to form sodium phenate (Abraham et al., 2020; Rocha et al., 2014).

#### 3.2.2. Oxidation of delignified corn cob

Periodate oxidation is noted for its ability to convert 1,2-dihydroxyl groups to dialdehyde groups. In this study, the maximum $NaIO_4$ consumption was achieved after 3 h of reaction. Initially, 100 mM $NaIO_4$ was offered per gram of delignified cellulose, of which approximately 82.32 % was consumed.

FT-IR analysis revealed differences between the spectrum of the pretreated corn cob support and that of the oxidized support (Fig. 4C). Although both spectra exhibited general similarities, noticeable changes were observed in the 2900 $cm^{-1}$ region, giving rise to a double-shouldered structure. This transformation is attributed to the extension of the aldehyde (CH) group in the 2910-2850 $cm^{-1}$ region, confirming the generation of new bonds in the fiber structure as a result of the oxidation process (Moreno Jaraba, 2012). In addition, at 1722 $cm^{-1}$ characteristic signals of C=O bonds appeared, corresponding to the aldehyde and carboxyl groups of the oxidized cellulose (Tang et al., 2017).

In the DSC analysis (Fig. 4A), a significant thermal transition was observed in oxidized cellulose, with a melting temperature of approximately 112.85 °C, higher than in non-oxidized cellulose. This increase in melting point is attributed to the higher flexibility of its molecular structure, obtaining in thermal stability due to the entanglement effect of flexible microfibers (Cao et al., 2012; Števulova et al., 2016). In addition, the higher thermal stability may be related to a possible increase in the degree of crystallinity of oxidized cellulose compared to delignified cellulose.

In the TGA was also used to study the thermal stability of the oxidized cellulose, as shown in the curve in Fig. 4B. The first thermal peak, observed at approximately 277.91 °C, was characterized by an average weight loss of 24.01 %. This weight loss, higher than that observed in delignified cellulose, is due to structural changes in the cellulose caused by the oxidation process. According to T. Zhang et al. (2017) this phenomenon is due to a decrease in cellulose morphology due to the opening of hydroxyl groups caused by the presence of aldehyde groups, which increases the susceptibility of oxidized cellulose to thermal degradation.

The second thermal event, with peaks at 401.44 and 402.56 °C, is associated with the decomposition of larger polymeric chains, reflecting the formation of additional bonds between the enzyme and cellulose. This 4.2 % weight loss indicates the presence of strong interactions, such as C-N bonds, which enhance the thermal stability of the immobilized material (Asmat et al., 2018; Maiti et al., 2013). This interaction is related to the immobilization of naringinase, where the aldehyde groups of the functionalized cellulose interact with the amino groups of the enzyme through covalent bonds, favoring the thermal stability of the system (Kalmouch et al., 2020).

### 3.3. Immobilization of commercial naringinase and purified naringinase from functionalized corncob

To evaluate the immobilization efficiency, aliquots were taken at different times and the amount of protein and enzyme activity present in the supernatant were calculated, as well as the enzyme activity of the immobilized enzymes. In this sense, NgseC and NgseP correspond to the enzyme in the supernatant, whose concentration decreases progressively due to its incorporation into the functionalized material (Fig. 5A and B). This behavior is evident in the decrease of enzyme activity in the supernatant over time, indicating the effective transfer of the enzyme to the immobilization support.

As a result of this process, NgseC IM and NgseP IM show an increase in enzyme activity, confirming the efficient retention of the enzyme on the support. NgsaP IM showed an efficiency of 85 % for activity and 87 % for protein determination by the Bradford method (Fig. 5A). NgsaC IM achieved an immobilization efficiency of 79 % after 90 min by enzyme activity and 83 % by Bradford's method as explained in section 2.5 (Fig. 5B) (Puri, 2012; D. Wang et al., 2019). The difference in immobilization efficiency between commercial and purified naringinase could be explained by the purification process to which the naringinase was subjected. This process focused on increasing the selectivity toward $\alpha$-L-rhamnosidase, which allowed the removal of contaminants and resulted in a higher binding capacity to the immobilization supports. In addition, the purification may have improved the structural conformation of the enzyme, facilitating its interaction with the supports and increasing its retention capacity (Barbosa et al., 2015; Martínez-Galán et al., 2021).

These findings are supported by the research (Zhou et al., 2021) which, purified naringinase with higher $\beta$-*D*-glucosidase activity showed an immobilization efficiency of 90.10 %, compared to 61.40 % for the unpurified enzyme. This suggests that purification of the enzyme can significantly increase its immobilization efficiency; this is in agreement with that obtained by (Puri et al., 2010) where commercial naringinase obtained an immobilization efficiency of 76 %, while purified naringinase with $\alpha$-*L*-rhamnosidase activity reached 80 %.

Immobilization was confirmed by FT-IR analysis within the following ranges: 350-4000 $cm^{-1}$, as shown in Fig. 4. In the spectrum, a peak near 1330 $cm^{-1}$ was identified, indicating the presence of cross-linking between the functionalized cellulose and naringinase, as described in Jacob and Suthindhiran (2020). It should be noted that the characteristic signal of the pure enzyme is evident in the range of 1645-1542 $cm^{-1}$, related to the vibrations of amide I and amide II (C=O stretching), and the spectrum with the immobilized enzyme. Changes slightly, indicating efficient binding between the enzyme and the support. In turn, according to Zdarta et al. (2015) these signals indicate that the enzyme can retain its activity. Finally, another characteristic signal was identified near 1700 $cm^{-1}$, corresponding to the stretching of the carbonyl (CO) group of the enzyme peptide.

#### 3.3.1. Stability of immobilized and purified commercial naringinase

The stability of the activity of immobilized NgsaC IM and NgsaP IM was determined by analyzing their activity at the time of immobilization (week 0) and subsequently at 2, 4, 6 and 8 weeks of storage at 4 °C (Fig. 5C). The results revealed that the immobilized enzymes retained more than 72 % of their relative activity even after 8 weeks of storage, this phenomenon could be attributed to the covalent binding of naringinase on the functionalized corn cob, which presents a stable structure throughout the storage period (Yu et al., 2021). These observations agreed with previous research (Borkar et al., 2021; Lei & Pan, 2012; Luo et al., 2019), which emphasize that the catalytic activity of immobilized naringinase remains constant even after a prolonged storage period. This result is of great significance, as the stability of the immobilized enzyme under prolonged storage conditions not only ensures its efficacy in long-term applications, but also reduces the costs associated with frequent enzyme replenishment in industrial processes (Mirsalami et al., 2024).

#### 3.3.2. Reutilization and stability of immobilized naringinase

A reusability of commercial and purified immobilized naringinase

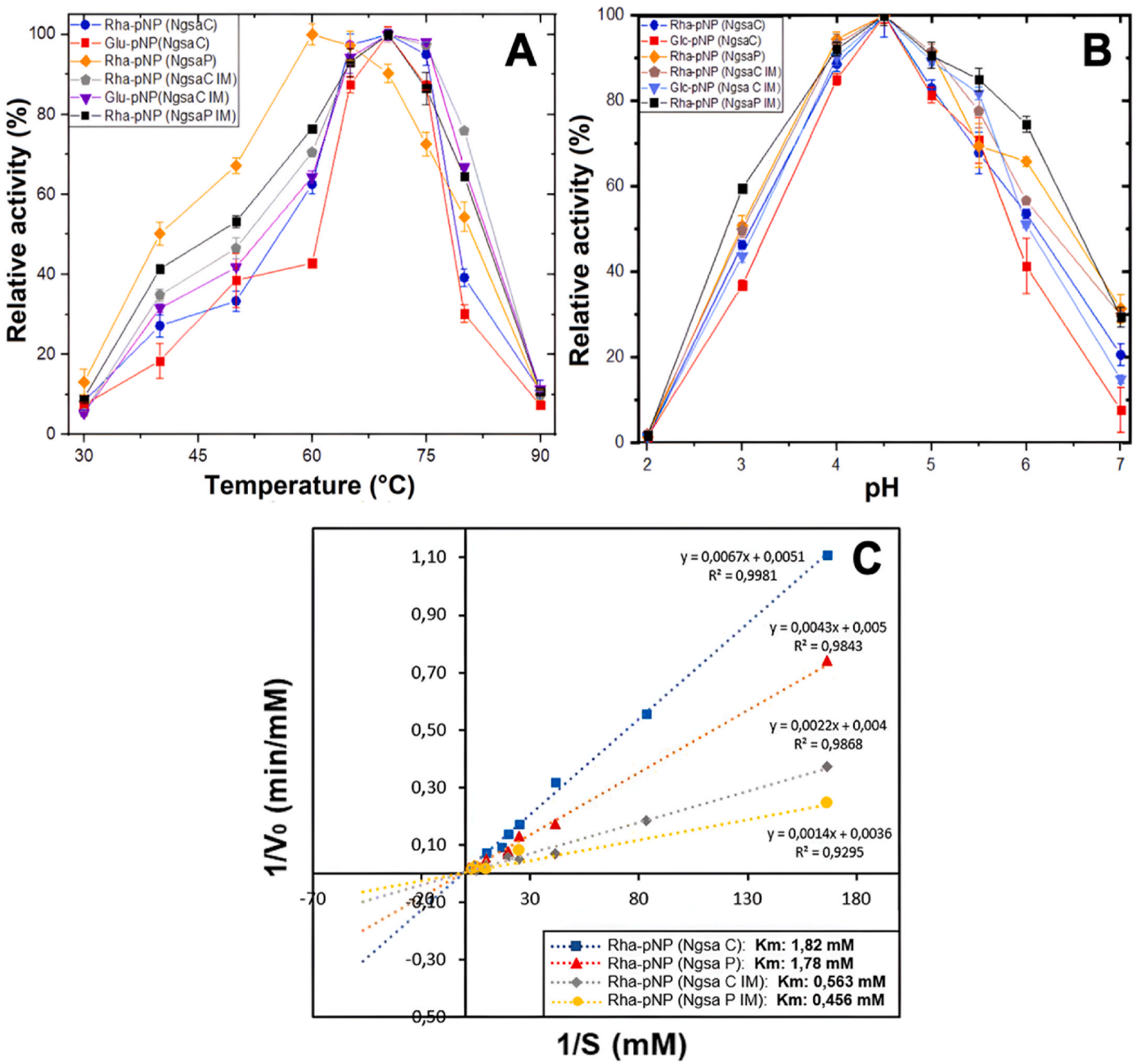



**Fig. 6.** Relative activity as a function of temperature for free and immobilized naringinase (A); relative activity as a function of pH for free and immobilized naringinase (B); Lineweaver-Burk plot of NgsaC- NgsaP and immobilized enzyme (C).

(Fig. 5D) is observed for 10 consecutive cycles without significant losses in enzyme activity for each cycle, suggesting high stability of the immobilized enzyme due to the covalent bonding. This study represents significant improvement over previous research on naringinase immobilization; for example (Puri et al., 2005), studied the immobilization of the enzyme by covalent bonding using glutaraldehyde-coated wood chips, achieving 7 reuses. This aspect is particularly relevant from the point of view of large-scale production of high-value prunin and naringenin (Victor et al., 2018).

### 3.3.3. *Influence of temperature on reaction rate*

The influence of temperature on the $\alpha$-L-rhamnosidase and $\beta$-D-glucosidase activities of naringinase in both free and immobilized (commercial and purified) forms was determined. The results presented in Fig. 6A show that both enzymes immobilized on the support exhibited optimal activity at 70 °C, similar to what was previously obtained by (Bodakowska-Boczniewicz & Garncarek, 2019, p. 4234). This optimum temperature is 10 °C higher for purified naringinase, suggesting a higher potential for industrial application, with 70 °C being the ideal temperature for citrus juice pasteurization (Oliveira et al., 2022; Luo et al., 2019; Yu et al., 2021).

This result is supported by previous research by (S. Liu et al., 2021; Z. Q. Liu et al., 2012) which has suggested that the increase in optimal temperature can be attributed to the formation of a Schiff base covalent bond during the immobilization process (Jamwal et al., 2019; Li et al., 2016). This bond confers rigidity to the enzyme, reducing its susceptibility to temperature-induced conformational changes (Jiang et al., 2017). The cleavage of the Schiff base bond to form an amine result in a broad increase in the operating temperature range, making the enzyme more thermophilic. This change is associated with the reduction of the

**Table 3**
$K_M$ values for naringinase in its free and immobilized form.

| Enzime | $K_M$ (mM) Free | Inmobilized | $CK_M$ | Support material | Ref |
|---|---|---|---|---|---|
| Naringinase *Penicillum decumbens* | 0.23 | 0.35 | 0.67 | Polyvinyl alcohol (PVA) | Nunes et al. (2010) |
| Naringinase *Penicillum decumbens* | 0.19 | 6.59 | 0.03 | Chitosan microspheres | Bodakowska-Boczniewicz and Garncarek (2019) |
| Naringinase *Penicillum decumbens* | 1.87 | 0.80 | 2.34 | Graphene oxide | Carceller et al. (2019). |
| Naringinase *Penicillum decumbens* | 1.8 | 0.61 | 2.95 | Graphene oxide | Carceller et al. (2019). |
| Naringinase *Penicillum decumbens* (commercial) | 1.82 | 0.56 | 3.25 | Corn cob powder | This work |
| Naringinase *Penicillum decumbens* (purified) | 1.78 | 0.46 | 3.86 | Corn cob powder | This work |

CH=N double bond to $CH_2$-NH, which brings flexibility to the structure and prevents its distortion.

### 3.3.4. Effect of pH on enzyme activity

The effect of pH on the enzymatic activity of immobilized naringinase (NgsaC and NgsaP) for the hydrolysis of Rha-*p*NP and Glu-*p*NP was determined over a pH range of 2.00–7.00. Fig. 6B shows that the pH optimum for both commercial, purified and immobilized enzymes was 4.50. This is because the pH optimum of an enzyme is determined primarily by the tertiary structure of the enzyme and the conformation it acquires three-dimensionally along with the electrical charge of the active groups within the molecule (Lei & Pan, 2012; Nunes et al., 2012); when an enzyme is immobilized, its tertiary structure may change slightly due to interaction with the solid support, but the active groups responsible for enzymatic activity generally do not change (Siddiqui, 2017; Yuan et al., 2023), which showed that the pH optimal activity remains the same as that of the free enzyme.

This finding is in agreement with previous studies by (Lei & Pan, 2012; Li et al., 2016; Nunes et al., 2012), which showed that the pH optimal activity is maintained equal to that of the free enzyme. Furthermore, it indicates that naringinase immobilized on corn cob powder is able to maintain high activity at a pH level similar to that of fruit juices (below pH: 5.00), suggesting a higher compatibility with industrial conditions.

These results have important implications because together with the optimal temperature of the immobilized enzymes work for applications in industrial processes. Furthermore, research has suggested that these compounds obtained by NgsaC IM and NgsaP IM have the ability to interact and be released in the colorectal tract and be preventive compounds for the prevention of colon cancer, since only a minimal fraction of these compounds are stored in the small intestine and the rest of the compounds (approximately 95 %) are metabolized and stored in the colon.

### 3.3.5. Determination of the Michaelis-Menten constant ($K_M$)

Determination of Michaelis-Menten constants (Fig. 6C) by the Lineweaver-Burk method showed significant differences between purified ($K_M$ = 1.78 mM) and commercial ($K_M$ = 1.82 mM) naringinase, highlighting the higher affinity of purified naringinase for the substrate Rha-*p*NP (Shilpa, Farha, et al., 2023), suggesting a higher catalytic capacity and selectivity towards *α-L*-rhamnosidase activity and prunin production. For immobilized enzymes, a remarkable decrease in $K_M$ values was observed between NgsaC IM (0.56 mM) and NgsaP IM (0.46 mM), indicating higher enzyme affinity towards the substrate after immobilization (Feng et al., 2024), probably due to increased exposure of the enzyme active sites as a result of covalent immobilization.

The reduction in $K_M$ after immobilization with naringinase agrees with previous research in similar studies with immobilized naringinase, Table 3 summarizes the $K_M$ values reported for naringinase in its free and immobilized state on different supports. For comparisons, the $CK_M$ ratio ($K_M$ of free enzyme divided by $K_M$ of immobilized naringinase) was calculated (Carceller et al., 2019) for the different supports used in the immobilization of naringinase. These results support the efficacy of this process in improving the catalytic properties of the enzymes; it is notable that the $CK_M$ values found for immobilized naringinase are higher than those previously reported, indicating a significant increase in substrate affinity after the immobilization process performed in this research.

**Table 4**
Antioxidant activity and selectivity towards *α-L*-rhamnosidase of different treatments of naringin and orange albedo extract hydrolyzed by immobilized enzymes.

| Treatment | DPPH (%) | Selectivity (%) |
|---|---|---|
| Commercial naringin **(N)** | 55.69 ± 2.22 | – |
| Commercial Naringin hydrolyzed by NgsaC IM **(Na)** | 91.25 ± 1.42 | 85 |
| Commercial naringin hydrolyzed by NgsaP IM **(aNa)** | 86.12 ± 1.54 | 90 |
| Orange albedo extract **(N*)** | 50.21 ± 2.53 | – |
| Orange albedo extract hydrolyzed by NgsaC IM **(Na*)** | 74.09 ± 3.51 | 82 |
| Orange albedo extract hydrolyzed by NgsaP IM **(aNa*)** | 68.52 ± 1.03 | 86 |

### 3.4. Evaluation of antioxidant activity: extracts obtained and hydrolyzed extracts

From a biological point of view, flavanones exhibit a variety of activities including antioxidant activities; they have demonstrated their potential usefulness in the treatment of cardiovascular diseases, neurodegenerative disorders and cancer. Most metabolic diseases are caused by oxidative stress, which highlights the importance of investigating the positive effects of flavanones and their antioxidant capacity by DPPH analysis (X. Wang et al., 2021).

Flavanones extracted from orange peel albedo include compounds such as naringin, narirutin, hesperidin, neohesperidin, and rutin, which exhibit variable antioxidant activity depending on their chemical structure. During enzymatic hydrolysis with naringinase, these compounds undergo elimination of their glycosidic groups, transforming into their respective aglycones (naringenin, eriocitrin, hesperetin, etc.), which possess higher antioxidant capacity due to their higher availability of free hydroxyl groups and better interaction with free radicals (Cheng et al., 2020; Khoo et al., 2017; Ramesh et al., 2021). In contrast, the commercial naringin used as a substrate in this study contains exclusively this single flavanone, which allows establishing a reference to compare the effects of enzymatic hydrolysis in a pure compound versus a natural extract with a more complex composition. This comparative analysis is essential to evaluate the efficiency of the enzymatic process and to develop strategies to improve the availability of bioactive compounds with antioxidant potential.

Table 4 shows that hydrolysis by NgsaC IM presented the highest DPPH radical scavenging ability, followed by hydrolysis by NgsaP IM. Although there is substrate competition and mutual inhibition between the *α-L*-rhamnosidase and *β-D*-glucosidase activities of naringinase, enzymatic hydrolysis significantly enhances the antioxidant activities. This effect is due to the release of aglycones with more reactive chemical structures, even though the selectivity towards *α-L*-rhamnosidase in the

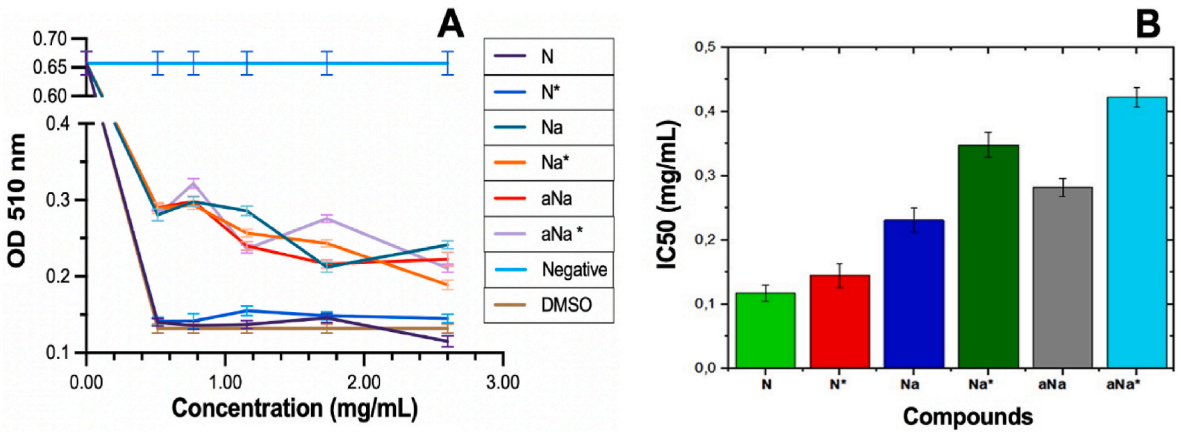



**Fig. 7.** Cell viability assay (A) and IC50 of cell model SW480 (B) for the compounds: Commercial naringin (N), commercial naringin hydrolyzed by NgsaC IM (Na), commercial naringin hydrolyzed by NgsaP IM (aNa), orange albedo extract (N*), orange albedo extract hydrolyzed by NgsaC IM (Na*), orange albedo extract hydrolyzed by NgsaP IM (aNa*) and positive controls DMSO and Negative (no treatment).

immobilized enzyme is 4 % lower compared to the purified enzyme (Ramesh et al., 2021).

These results are in agreement with the antioxidant capacity of polyphenols and the number of hydroxyl groups on the aromatic rings, the chemical structure of phenols, the position of hydroxyl groups and the glycosylation of these (Xie et al., 2015). Compared to their corresponding aglycones, glycosylated flavanones generally show lower antioxidant capacity. This activity decreases with increasing number of glycosidic residues, with both the position and structure of the sugars being important factors (Slámová et al., 2018, p. 2126).

### *3.4.1. Biological potential of flavanones obtained from orange peels*

Naringin (N) and the extract obtained from orange peel (N*) exhibited a concentration-dependent cell inhibition effect on SW480 cells at 48 h (Fig. 7A). The highest cell death effect was observed with commercial naringin and the extract obtained from orange albedo, as is shown in Fig. 7B. Commercial naringin showed the greatest reduction in cell viability (IC50: 0.117 mg/mL), followed by the orange albedo extract (IC50: 0.145 mg/mL).

In addition, there was a considerable decrease in viability induced by NgsaC IM hydrolyzed naringin (Na) and its extract (Na*), with Na showing a greater effect (IC50: 0.231 mg/mL) compared to Na* (IC50: 0.349 mg/mL). A similar pattern was also observed with NgsaP IM-hydrolyzed naringin (aNa) and its corresponding extract (aNa*), where aNa exhibits a lower IC50 in cell viability (IC50: 0.282 mg/mL) compared to aNa* (IC50: 0.423 mg/mL) (Fig. 7B). These results suggest that both hydrolyzed extracts of commercial substrate exhibit significant cytotoxic effect on SW480 cells.

These results are consistent with previous (Ghanbari-Movahed et al., 2021; Yoshinaga et al., 2016; Yu et al., 2021) that demonstrated the mechanism of naringin-induced cell death. This mechanism is explained by activation of caspase-3, an enzyme central in the execution of programmed cell death, modulation of anti-apoptotic proteins such as Bcl-2 and promotion of cytochrome C release from mitochondria. In addition, it will be observed that the orange albedo compound also exhibited significant inhibitory effects, suggesting a potential added value in the use of substrates obtained from waste.

## 4. Conclusions

The purification of naringinase resulted in a significant increase in *α-L*-rhamnosidase activity, highlighting a simple, practical and feasible methodology as a strategy to improve the functional properties of the enzyme, with important implications in the selective production of compounds such as prunin.

Immobilization of commercial and purified naringinase on functionalized corn cob was successfully carried out, confirmed by its enzymatic activity and physicochemical characterizations; this immobilization resulted in higher thermal stability and higher enzymatic affinity towards the substrate, as evidenced by TGA, DSC analysis and determination of Michaelis-Menten constant ($K_M$), temperature and pH. This biocatalyst can sustain up to 10 consecutive cycles; which is relevant for large-scale production of high value-added compounds from agro-industrial wastes.

Enzymatic hydrolysis of flavanones demonstrated high antioxidant capacity and a significant decrease in cell viability in the SW480 colon cancer model. A marked reduction in cell viability was observed after treatment with hydrolyzed flavanones, with a more evident impact at 48 h. The results indicate that naringin hydrolyzed by NgsaC IM presented the lowest IC50, suggesting a potential added value when using substrates obtained from agro-industrial waste.

## CRediT authorship contribution statement

**Kevin Esteban Garzón-Alonso:** Writing – review & editing, Writing – original draft, Validation, Methodology, Investigation, Formal analysis, Data curation, Conceptualization. **Maryli Jessenia Bohorquez-Peña:** Writing – review & editing, Formal analysis. **Brandon Vargas-Suaza:** Writing – review & editing, Formal analysis, Data curation. **Julio Cesar Rendón-Londoño:** Writing – review & editing, Methodology, Investigation, Formal analysis, Conceptualization. **Mónica Mesa:** Writing – review & editing, Formal analysis, Conceptualization. **Yuly Nataly Franco-Tobón:** Writing – review & editing, Formal analysis, Conceptualization. **Julián Paul Martínez-Galán:** Writing – review & editing, Writing – original draft, Visualization, Validation, Supervision, Project administration, Methodology, Investigation, Funding acquisition, Formal analysis, Data curation, Conceptualization.

## Declaration of competing interest

The authors declare that they have no known competing financial interests or personal relationships that could have appeared to influence the work reported in this paper.

## Acknowledgments

This research was supported by Sistema General de Regalías (SGR, General Royalties System) in the 7th call of the Ministry of Science, Technology and Innovation MinCiencias-Colombia. The authors thank the University of Antioquia and some of its research groups for their

different contributions, GIANH (Human Feeding and Nutrition Research Group), the CIENMATE laboratory (Materials Sciences), GENMOL (Molecular Genetics Group), and the GRC laboratory (Genetics, Regeneration and Cancer).

## Appendix A. Supplementary data

Supplementary data to this article can be found online at https://doi.org/10.1016/j.fbio.2025.106752.

## Data availability

Data will be made available on request.

## References


Abraham, A., Mathew, A. K., Park, H., Choi, O., Sindhu, R., Parameswaran, B., Pandey, A., Park, J. H., & Sang, B. I. (2020). Pretreatment strategies for enhanced biogas production from lignocellulosic biomass. *Bioresource Technology, 301*, Article 122725. https://doi.org/10.1016/J.BIORTECH.2019.122725

Ahmed, O. M., Hassan, M. A., Abdel-Twab, S. M., & Abdel Azeem, M. N. (2017). Navel orange peel hydroethanolic extract, naringin and naringenin have anti-diabetic potentials in type 2 diabetic rats. *Biomedicine & Pharmacotherapy, 94*, 197–205. https://doi.org/10.1016/J.BIOPHA.2017.07.094

Asmat, S., Husain, Q., & Khan, M. S. (2018). A polypyrrole-methyl anthranilate functionalized worm-like titanium dioxide nanocomposite as an innovative tool for immobilization of lipase: Preparation, activity, stability and molecular docking investigations. *New Journal of Chemistry, 42*(1), 91–102. https://doi.org/10.1039/C7NJ02951A

Barbosa, O., Ortiz, C., Berenguer-Murcia, Á., Torres, R., Rodrigues, R. C., & Fernandez-Lafuente, R. (2015). Strategies for the one-step immobilization–purification of enzymes as industrial biocatalysts. *Biotechnology Advances, 33*(5), 435–456. https://doi.org/10.1016/J.BIOTECHADV.2015.03.006

Bassan, J. C., Bezerra, T. M. de S., Peixoto, G., da Cruz, C. Z. P., Galán, J. P. M., Vaz, A. B., dos, S., Garrido, S. S., Filice, M., & Monti, R. (2016). Immobilization of trypsin in lignocellulosic waste material to produce peptides with bioactive potential from whey protein. *Materials, 9*(5), 357. https://doi.org/10.3390/MA9050357

Bodakowska-Boczniewicz, J., & Garncarek, Z. (2019). Immobilization of naringinase from Penicillium decumbens on chitosan microspheres for debittering grapefruit juice. *Molecules, 24*(23), 4234. https://doi.org/10.3390/MOLECULES24234234

Bodakowska-Boczniewicz, J., & Garncarek, Z. (2022). Naringinase biosynthesis by Aspergillus Niger on an optimized medium containing red grapefruit albedo. *Molecules, 27*(24), 8763. https://doi.org/10.3390/MOLECULES27248763

Borkar, V., Chakraborty, S., & Gokhale, J. S. (2021). Fermentative production of naringinase from Aspergillus Niger van Tieghem MTCC 2425 using citrus wastes: Process optimization, partial purification, and characterization. *Applied Biochemistry and Biotechnology, 193*(5), 1321–1337. https://doi.org/10.1007/S12010-020-03385-9/FIGURES/3

Borzova, N. V. (2023). Microbial α-L-rhamnosidases: classification, distribution, properties and practical application. *Biotechnologia Acta, 16*(4), 5–21. https://doi.org/10.15407/BIOTECH16.04.005

Bradford, M. M. (1976). A rapid and sensitive method for the quantitation of microgram quantities of protein utilizing the principle of protein-dye binding. *Analytical Biochemistry, 72*(1–2), 248–254. https://doi.org/10.1016/0003-2697(76)90527-3

Cao, X., Ding, B., Yu, J., & Al-Deyab, S. S. (2012). Cellulose nanowhiskers extracted from TEMPO-oxidized jute fibers. *Carbohydrate Polymers, 90*(2), 1075–1080. https://doi.org/10.1016/J.CARBPOL.2012.06.046

Carceller, J. M., Martínez Galán, J. P., Monti, R., Bassan, J. C., Filice, M., Iborra, S., Yu, J., & Corma, A. (2019). Selective synthesis of citrus flavonoids prunin and naringenin using heterogeneized biocatalyst on graphene oxide. *Green Chemistry, 21*(4), 839–849. https://doi.org/10.1039/C8GC03661F

Carceller, J. M., Martínez Galán, J. P., Monti, R., Bassan, J. C., Filice, M., Yu, J., Climent, M. J., Iborra, S., & Corma, A. (2020). Covalent immobilization of naringinase over two-dimensional 2D zeolites and its applications in a continuous process to produce citrus flavonoids and for debittering of juices. *ChemCatChem, 12*(18), 4502–4511. https://doi.org/10.1002/CCTC.202000320

Chang, H. Y., Lee, Y. B., Bae, H. A., Huh, J. Y., Nam, S. H., Sohn, H. S., Lee, H. J., & Lee, S. B. (2011). Purification and characterisation of Aspergillus sojae naringinase: The production of prunin exhibiting markedly enhanced solubility with *in vitro* inhibition of HMG-CoA reductase. *Food Chemistry, 124*(1), 234–241. https://doi.org/10.1016/J.FOODCHEM.2010.06.024

Cheng, C., Jia, M., Gui, Y., & Ma, Y. (2020). Comparison of the effects of novel processing technologies and conventional thermal pasteurisation on the nutritional quality and aroma of Mandarin (Citrus unshiu) juice. *Innovative Food Science & Emerging Technologies, 64*, Article 102425. https://doi.org/10.1016/J.IFSET.2020.102425

Chi, H., Cong Duong, T., Trung Hao, V., Thuy Khanh Linh, D., Van Nhat, H., Thi Hong Nhu, P., Nguyen Tuong Vy, V., Tan Cuong, L., Thanh Phong, L., & Tan Dung, N. (2018). Study and manufacture of the low temperature vacuum drying system in pillot scale. *Journal of Technical Education Science, 13*(4), 1–8. https://jte.edu.vn/index.php/jte/article/view/252.

da Silva, C. M. G., Contesini, F. J., Sawaya, A. C. H. F., Cabral, E. C., da Silva Cunha, I. B., Eberlin, M. N., & de Oliveira Carvalho, P. (2013). Enhancement of the antioxidant activity of orange and lime juices by flavonoid enzymatic de-glycosylation. *Food Research International, 52*(1), 308–314. https://doi.org/10.1016/J.FOODRES.2013.03.019

de Oliveira, F., Castellane, T. C. L., de Melo, M. R., & Buzato, J. B. (2022). Preparation of Aspergillus Niger 426 naringinases for debittering citrus juice utilization of agro-industrial residues. *International Microbiology, 25*(1), 123–131. https://doi.org/10.1007/S10123-021-00199-5/TABLES/3

Fang, X., Dong, Y., Xie, Y., Wang, L., Wang, J., Liu, Y., Zhao, L., & Cao, F. (2019). Effects of β-glucosidase and α-rhamnosidase on the contents of flavonoids, ginkgolides, and aroma components in ginkgo tea drink. *Molecules, 24*(10), 2009. https://doi.org/10.3390/MOLECULES24102009

Feng, T., Shi, J., Xia, J., Ren, X., Adesanya, O. I., Suo, H., & Zou, B. (2024). Lipase in-situ immobilized in covalent organic framework: Enzymatic properties and application in the preparation of 1, 3-dioleoyl-2-palmitoylglycerol. *Colloids and Surfaces B: Biointerfaces, 238*, Article 113873. https://doi.org/10.1016/J.COLSURFB.2024.113873

Ferreira, L. R., Macedo, J. A., Ribeiro, M. L., & Macedo, G. A. (2013). Improving the chemopreventive potential of orange juice by enzymatic biotransformation. *Food Research International, 51*(2), 526–535. https://doi.org/10.1016/J.FOODRES.2013.01.018

Foreign Agricultural Service (FAS). (2022). *Global markets for Texas oranges 1*.

Ghanbari-Movahed, M., Jackson, G., Farzaei, M. H., & Bishayee, A. (2021). A systematic review of the preventive and therapeutic effects of naringin against human malignancies. *Frontiers in Pharmacology, 12*, Article 639840. https://doi.org/10.3389/FPHAR.2021.639840/BIBTEX

Gobernación del Tolima. (2021). *Plan de Desarrollo Departamental*. El Tolima nos une 2020-2023.

Gomes, A. L., Petrus, R. R., de Sousa, R. L. M., & Fernandes, A. M. (2024). Aflatoxins and fumonisins in conventional and organic corn: A comprehensive review. *Food Additives & Contaminants: Part A, 41*(5), 575–586. https://doi.org/10.1080/19440049.2024.2330092

González, Y., Ortega, N., & Busto, M. (2020). Optimización de la inmovilización de naringinasa en criogeles de alcohol polivinílico y polietilenglicol. *Informacion Tecnologica, 31*(1), 29–40. https://go.gale.com/ps/i.do?p=IFME&sw=w&issn=07168756&v=2.1&it=r&id=GALE%7CA621405740&sid=googleScholar&linkaccess=fulltext.

Hasni, S., Rigane, G., Ghazghazi, H., Riguene, H., Bouallegue, A., Khedher, O., Oueslati, M. A., & Ben Salem, R. (2021). Optimum conditions and LC-ESI-MS analysis of phenolic rich extract from Eucalyptus marginata L. Under maceration and ultrasound-assisted extraction methods using response surface methodology. *Journal of Food Quality, 2021*. https://doi.org/10.1155/2021/5591022

Jackson, E., Correa, S., & Betancor, L. (2019). Cellulose-based nanosupports for enzyme immobilization, 1235–1253 https://doi.org/10.1007/978-3-319-77830-3_42.

Jacob, J. J., & Suthindhiran, K. (2020). Immobilisation of lipase enzyme onto bacterial magnetosomes for stain removal. *Biotechnology Reports, 25*. https://doi.org/10.1016/J.BTRE.2020.E00422

Jamwal, S., Dautoo, U. K., Ranote, S., Dharela, R., & Chauhan, G. S. (2019). Enhanced catalytic activity of new acryloyl crosslinked cellulose dialdehyde-nitrilase Schiff base and its reduced form for nitrile hydrolysis. *International Journal of Biological Macromolecules, 131*, 117–126. https://doi.org/10.1016/J.IJBIOMAC.2019.03.034

Jiang, W., Tao, R., Yang, Y., Xu, Y., Kang, H., Zhou, X., & Zhou, Z. (2017). Production of (R)-(−)-mandelic acid with nitrilase immobilized on D155 resin modified by l-lysine. *Biochemical Engineering Journal, 127*, 32–42. https://doi.org/10.1016/J.BEJ.2017.07.010

Kalmouch, A., El-Sakhawy, M., Kamel, S., Salama, A., & Hesemann, P. (2020). A green method for preparation of amino acids functionalized 2,3-dialdehyde cellulose. *Egyptian Journal of Chemistry, 63*(9), 3517–3532. https://doi.org/10.21608/EJCHEM.2020.22552.2341

Kang, C. H., Rhie, S. J., & Kim, Y. C. (2018). Antioxidant and skin anti-aging effects of marigold methanol extract. *Toxicological Research, 34*(1), 31–39. https://doi.org/10.5487/TR.2018.34.1.031/METRICS

Kapešová, J., Petrásková, L., Markošová, K., Rebroš, M., Kotik, M., Bojarová, P., & Křen, V. (2019). Bioproduction of quercetin and rutinose catalyzed by rutinosidase: Novel concept of "solid state biocatalysis.". *International Journal of Molecular Sciences, 20*(5), 1112. https://doi.org/10.3390/IJMS20051112

Karamitros, C. S., Murray, K., Kumada, Y., Johnson, K. A., D'Arcy, S., & Georgiou, G. (2024). Mechanistic conformational and substrate selectivity profiles emerging in the evolution of enzymes via parallel trajectories. *Nature Communications, 15*(1), 1–17. https://doi.org/10.1038/s41467-024-51133-y

Kenney, K. L., Smith, W. A., Gresham, G. L., & Westover, T. L. (2013). Understanding biomass feedstock variability. *Biofuels, 4*(1), 111–127. https://doi.org/10.4155/BFS.12.83

Khalid, K. A., Ahmad, A. A., & Yong, T. L.-K. (2017). Lignin extraction from lignocellulosic biomass using Sub- and supercritical Fluid technology as precursor for Carbon fiber production. *Journal of the Japan Institute of Energy, 96*(8), 255–260. https://doi.org/10.3775/JIE.96.255

Khoo, H. E., Azlan, A., Tang, S. T., & Lim, S. M. (2017). Anthocyanidins and anthocyanins: Colored pigments as food, pharmaceutical ingredients, and the potential health benefits. *Food & Nutrition Research, 61*(1). https://doi.org/10.1080/16546628.2017.1361779

Kim, C., Park, J., Lee, H., Hwang, D. Y., Park, S. H., & Lee, H. (2022). Evaluation of the EtOAc extract of lemongrass (cymbopogon citratus) as a potential skincare cosmetic material for acne vulgaris. *Journal of Microbiology and Biotechnology, 32*(5), 594. https://doi.org/10.4014/JMB.2201.01037

Kumar, S., & Pandey, A. K. (2013). Chemistry and biological activities of flavonoids: An overview. *The Scientific World Journal, 2013*. https://doi.org/10.1155/2013/162750

Lei, S., & Pan, S. (2012). Improvement of the activity of naringinase by covalent immobilization on sodium alginate in biomaterial engineering and its applications. *Advanced Materials Research, 578*, 187–190. https://doi.org/10.4028/WWW.SCIENTIFIC.NET/AMR.578.187

Li, Q., Wang, Y., Zhang, L., Chen, L., Du, Y., Ye, T., & Shi, X. (2016). Naringenin exerts anti-angiogenic effects in human endothelial cells: Involvement of ERRα/VEGF/KDR signaling pathway. *Fitoterapia, 111*, 78–86. https://doi.org/10.1016/J.FITOTE.2016.04.015

Li, Q., Zhang, N., Sun, X., Zhan, H., Tian, J., Fei, X., Liu, X., Chen, G., & Wang, Y. (2021). Controllable biotransformation of naringin to prunin by naringinase immobilized on functionalized silica. *Journal of Chemical Technology & Biotechnology, 96*(5), 1218–1227. https://doi.org/10.1002/JCTB.6634

Liu, S., Bilal, M., Rizwan, K., Gul, I., Rasheed, T., & Iqbal, H. M. N. (2021). Smart chemistry of enzyme immobilization using various support matrices – a review. *International Journal of Biological Macromolecules, 190*, 396–408. https://doi.org/10.1016/J.IJBIOMAC.2021.09.006

Liu, Z. Q., Zhou, M., Zhang, X. H., Xu, J. M., Xue, Y. P., & Zheng, Y. G. (2012). Biosynthesis of iminodiacetic acid from iminodiacetonitrile by immobilized recombinant Escherichia coli harboring nitrilase. *Journal of Molecular Microbiology and Biotechnology, 22*(1), 35–47. https://doi.org/10.1159/000337055

Londoño, M. B. Z., Casabianca, G. A. L., Landazuri, P., Varela, S. S. A., & Celis, M. E. M. (2023). Aqueous extract of Andean berry (Vaccinium meridionale Swartz) promotes antiproliferative effect of 5-fluorouracil and leucovorin treatment with or without oxaliplatin and inhibits metastatic potential in colon adenocarcinoma cells. *Revista Colombiana de Cancerología, 27*(4), 433–442. https://doi.org/10.35509/01239015.979

Luo, J., Li, Q., Sun, X., Tian, J., Fei, X., Shi, F., Zhang, N., & Liu, X. (2019). The study of the characteristics and hydrolysis properties of naringinase immobilized by porous silica material. *RSC Advances, 9*(8), 4514–4520. https://doi.org/10.1039/C9RA00075E

Maceda, A., Soto-Hernández, M., Peña-Valdivia, C. B., Trejo, C., Terrazas, T., Maceda, A., Soto-Hernández, M., Peña-Valdivia, C. B., Trejo, C., & Terrazas, T. (2021). Lignina: Composición, síntesis y evolución. *Madera y Bosques, 27*(2). https://doi.org/10.21829/MYB.2021.2722137

Maiti, S., Jayaramudu, J., Das, K., Reddy, S. M., Sadiku, R., Ray, S. S., & Liu, D. (2013). Preparation and characterization of nano-cellulose with new shape from different precursor. *Carbohydrate Polymers, 98*(1), 562–567. https://doi.org/10.1016/J.CARBPOL.2013.06.029

Manzanares, P., de Graaff, L. H., & Visser, J. (1997). Purification and characterization of an α-l-rhamnosidase from Aspergillus Niger. *FEMS Microbiology Letters, 157*(2), 279–283. https://doi.org/10.1111/J.1574-6968.1997.TB12785.X

Martín-García, B., De Montijo-Prieto, S., Jiménez-Valera, M., Carrasco-Pancorbo, A., Ruiz-Bravo, A., Verardo, V., & Gómez-Caravaca, A. M. (2022). Comparative extraction of phenolic compounds from olive leaves using a sonotrode and an ultrasonic bath and the evaluation of both antioxidant and antimicrobial activity. *Antioxidants, 11*(3), 558. https://doi.org/10.3390/ANTIOX11030558/S1

Martínez-Galán, J. P., Ontibón-Echeverri, C. M., Campos Costa, M., Batista-Duharte, A., Guerso Batista, V., Mesa, V., Monti, R., Veloso de Paula, A., & Martins Baviera, A. (2021). Enzymatic synthesis of capric acid-rich structured lipids and their effects on mice with high-fat diet-induced obesity. *Food Research International, 148*, Article 110602. https://doi.org/10.1016/J.FOODRES.2021.110602

Méndez, P. A., Méndez, Á. M., Martínez, L. N., Vargas, B., & López, B. L. (2022). Cassava and banana starch modified with maleic anhydride-poly (ethylene glycol) methyl ether (Ma-mPEG): A comparative study of their physicochemical properties as coatings. *International Journal of Biological Macromolecules, 205*, 1–14. https://doi.org/10.1016/J.IJBIOMAC.2022.02.053

Miller, G. L. (1959). Use of dinitrosalicylic acid reagent for determination of reducing sugar. *Analytical Chemistry, 31*(3), 426–428. https://doi.org/10.1021/AC60147A030/ASSET/AC60147A030.FP.PNG_V03

Ministerio de Agricultura. (2024). Sistemas de estadísticas agropecuarias. Obtenido de Agronet: MinisteriodeAgricultura. (2024). Sistemas de estadísticas agropecuarias. Obtenido de Agronet: http://www.agronet.gov.co/Paginas/inicio.aspx.

Mirsalami, S. M., Mirsalami, M., & Ghodousian, A. (2024). Techniques for immobilizing enzymes to create durable and effective biocatalysts. *Results in Chemistry, 7*, Article 101486. https://doi.org/10.1016/J.RECHEM.2024.101486

Morán, J. I., Alvarez, V. A., Cyras, V. P., & Vázquez, A. (2008). Extraction of cellulose and preparation of nanocellulose from sisal fibers. *Cellulose, 15*(1), 149–159. https://doi.org/10.1007/S10570-007-9145-9/FIGURES/10

Moreno Jaraba, D. I. (2012). Efecto del tratamiento alcalino y explosión de vapor alcalino sobre las propiedades de la fibra de Cumare y su interface con una matriz de PLA. *Uniandes*. http://hdl.handle.net/1992/11580.

Nunes, M. A. P., Fernandes, P. C. B., & Ribeiro, M. H. L. (2012). High-affinity water-soluble system for efficient naringinase immobilization in polyvinyl alcohol–dimethyl sulfoxide lens-shaped particles. *Journal of Molecular Recognition, 25*(11), 580–594. https://doi.org/10.1002/JMR.2197

Nunes, M. A. P., Vila-Real, H., Fernandes, P. C. B., & Ribeiro, M. H. L. (2010). Immobilization of naringinase in PVA-alginate matrix using an innovative technique. *Applied Biochemistry and Biotechnology, 160*(7), 2129–2147. https://doi.org/10.1007/S12010-009-8733-6

Ortiz, D. L., Batuecas, E., Orrego, C. E., Rodríguez, L. J., Camelin, E., & Fino, D. (2020). Sustainable management of peel waste in the small-scale orange juice industries: A Colombian case study. *Journal of Cleaner Production, 265*, Article 121587. https://doi.org/10.1016/J.JCLEPRO.2020.121587

Pereira, R. M. S., López, B. G.-C., Diniz, S. N., Antunes, A. A., Garcia, D. M., Oliveira, C. R., & Marcucci, M. C. (2017). Quantification of flavonoids in Brazilian orange peels and industrial orange juice processing wastes. *Agricultural Sciences, 8*(7), 631–644. https://doi.org/10.4236/AS.2017.87048

Permata, D. A., Kasim, A., Asben, A., Yusniwati, Permata, D. A., Kasim, A., Asben, A., & Yusniwati. (2021). *Delignification of Lignocellulosic Biomass, 12*(2), 462–469. https://doi.org/10.30574/WJARR.2021.12.2.0618. https://Wjarr.Com/Sites/Default/Files/WJARR-2021-0618.Pdf

Pietricola, G., Ottone, C., Fino, D., & Tommasi, T. (2020). Enzymatic reduction of CO2 to formic acid using FDH immobilized on natural zeolite. *Journal of CO2 Utilization, 42*, Article 101343. https://doi.org/10.1016/J.JCOU.2020.101343

Puri, M. (2012). Updates on naringinase: Structural and biotechnological aspects. *Applied Microbiology and Biotechnology, 93*(1), 49–60. https://doi.org/10.1007/S00253-011-3679-3/FIGURES/3

Puri, M., Kaur, H., & Kennedy, J. F. (2005). Covalent immobilization of naringinase for the transformation of a flavonoid. *Journal of Chemical Technology & Biotechnology, 80*(10), 1160–1165. https://doi.org/10.1002/JCTB.1303

Puri, M., Kaur, A., Singh, R. S., Schwarz, W. H., & Kaur, A. (2010). One-step purification and immobilization of His-tagged rhamnosidase for naringin hydrolysis. *Process Biochemistry, 45*(4), 451–456. https://doi.org/10.1016/J.PROCBIO.2009.11.001

Ramesh, P., Jagadeesan, R., Sekaran, S., Dhanasekaran, A., & Vimalraj, S. (2021). Flavonoids: Classification, function, and molecular mechanisms involved in bone remodelling. *Frontiers in Endocrinology, 12*, Article 779638. https://doi.org/10.3389/FENDO.2021.779638/BIBTEX

Rashid, R., Wani, S. M., Manzoor, S., Masoodi, F. A., & Dar, M. M. (2022). Improving oxidative stability of edible oils with nanoencapsulated orange peel extract powder during accelerated shelf life storage. *Food Bioscience, 49*, Article 101917. https://doi.org/10.1016/J.FBIO.2022.101917

Rezzadori, K., Benedetti, S., & Amante, E. R. (2012). Proposals for the residues recovery: Orange waste as raw material for new products. *Food and Bioproducts Processing, 90*(4), 606–614. https://doi.org/10.1016/J.FBP.2012.06.002

Riseh, R. S., Vazvani, M. G., Hassanisaadi, M., & Thakur, V. K. (2024). Agricultural wastes: A practical and potential source for the isolation and preparation of cellulose and application in agriculture and different industries. *Industrial Crops and Products, 208*, Article 117904. https://doi.org/10.1016/J.INDCROP.2023.117904

Rocha, G. J. M., Nascimento, V. M., Silva, V. F. N. da, Corso, D. L. S., & Gonçalves, A. R. (2014). Contributing to the environmental sustainability of the second generation ethanol production: Delignification of sugarcane bagasse with sodium hydroxide recycling. *Industrial Crops and Products, 59*, 63–68. https://doi.org/10.1016/J.INDCROP.2014.05.002

Rocha-Meneses, L., Raud, M., Orupõld, K., & Kikas, T. (2017). Second-generation bioethanol production: A review of strategies for waste valorisation. *Agronomy Research, 15*(3), 830–847.

Romero, C. L., Mejía, H. C., Sánchez, Z. A., Balagurusamy, N., & Luévanos, E. M. (2014). Aplicaciones de las Enzimas Inmovilizadas. *Revista Científica de la Universidad Autónoma de Coahuila, 6*(11), 1–9.

Safdar, M. N., Kausar, T., Jabbar, S., Mumtaz, A., Ahad, K., & Saddozai, A. A. (2017). Extraction and quantification of polyphenols from kinnow (Citrus reticulate L.) peel using ultrasound and maceration techniques. *Journal of Food and Drug Analysis, 25*(3), 488–500. https://doi.org/10.1016/J.JFDA.2016.07.010

Sawalha, S. M. S., Arráez-Román, D., Segura-Carretero, A., & Fernández-Gutiérrez, A. (2009). Quantification of main phenolic compounds in sweet and bitter orange peel using CE–MS/MS. *Food Chemistry, 116*(2), 567–574. https://doi.org/10.1016/J.FOODCHEM.2009.03.003

Seong, H. J., Im, A. E., Kim, H., Park, N., Yang, K. Y., Kim, D., & Nam, S. H. (2023). Production of prunin and naringenin by using naringinase from Aspergillus oryzae NYO-2 and their neuroprotective properties and debitterization. *Journal of Agricultural and Food Chemistry, 71*(3), 1655–1666. https://doi.org/10.1021/ACS.JAFC.2C06586/SUPPL_FILE/JF2C06586_SI_001.PDF

Shilpa, V. S., Farha, R., Sreerag, N. K., Gopalakrishnan, K., & Shahada, C. (2023). Debittering citrus fruit juices, advances in immobilized enzyme technology: A review. *The Pharma Innovation Journal, 12*(5), 3096–3101. https://www.thepharmajournal.com/archives/?year=2023&vol=12&issue=5&ArticleId=20294.

Shilpa, V. S., Shams, R., Dash, K. K., Pandey, V. K., Dar, A. H., Ayaz Mukarram, S., Harsányi, E., & Kovács, B. (2023). Phytochemical properties, extraction, and pharmacological benefits of naringin: A review. *Molecules, 28*(15), 5623. https://doi.org/10.3390/MOLECULES28155623

Siddiqui, K. S. (2017). Defying the activity–stability trade-off in enzymes: Taking advantage of entropy to enhance activity and thermostability. *Critical Reviews in Biotechnology, 37*(3), 309–322. https://doi.org/10.3109/07388551.2016.1144045

Slámová, K., Kapešová, J., & Valentová, K. (2018). "Sweet flavonoids": Glycosidase-catalyzed modifications. *International Journal of Molecular Sciences 2018, 19*(7), 2126. https://doi.org/10.3390/IJMS19072126

Števulova, N., Hospodárova, V., & Eštoková, A. (2016). Study of thermal analysis of selected cellulose fibres. *GeoScience Engineering, 62*(3), 18–21. https://doi.org/10.1515/GSE-2016-0020

Tang, Z., Li, W., Lin, X., Xiao, H., Miao, Q., Huang, L., Chen, L., & Wu, H. (2017). TEMPO-oxidized cellulose with high degree of oxidation. *Polymers, 9*(9), 421. https://doi.org/10.3390/POLYM9090421

Tayyab, M., Noman, A., Islam, W., Waheed, S., Arafat, Y., Ali, F., Zaynab, M., Lin, S., Zhang, H., & Lin, W. (2018). Bioethanol production from lignocellulosic biomass by environment-friendly pretreatment methods: A review. *Applied Ecology and Environmental Research, 16*(1), 225–249. https://doi.org/10.15666/AEER/1601_225249

Tobón, J. F. (2020). Recent advances and comparisons of conventional and alternative extraction techniques of phenolic compounds. *Journal of Food Science and Technology, 57*(12), 4299–4315. https://doi.org/10.1007/S13197-020-04433-2/

Valdés, A., Beltrán, A., Karabagias, I., Badeka, A., Kontominas, M. G., & Garrigós, M. C. (2015). Monitoring the oxidative stability and volatiles in blanched, roasted and fried almonds under normal and accelerated storage conditions by DSC, thermogravimetric analysis and ATR-FTIR. *European Journal of Lipid Science and Technology, 117*(8), 1199–1213. https://doi.org/10.1002/EJLT.201400384

Veeramachineni, A. K., Sathasivam, T., Muniyandy, S., Janarthanan, P., Langford, S. J., & Yan, L. Y. (2016). Optimizing extraction of cellulose and synthesizing pharmaceutical grade carboxymethyl sago cellulose from Malaysian sago pulp. *Applied Sciences, 6*(6), 170. https://doi.org/10.3390/APP6060170

Victor, M. M., David, J. M., Sakukuma, M. C. K., França, E. L., & Nunes, A. V. J. (2018). A simple and efficient process for the extraction of naringin from grapefruit peel waste. *Green Processing and Synthesis, 7*(6), 524–529. https://doi.org/10.1515/GPS-2017-0112/MACHINEREADABLECITATION/RIS

Waghmare, R. B., Choudhary, P., Moses, J. A., Anandharamakrishnan, C., & Stapley, A. G. F. (2022). Trends in approaches to assist freeze-drying of food: A cohort study on innovations. *Food Reviews International, 38*(S1), 552–573. https://doi.org/10.1080/87559129.2021.1875232

Wang, X., Cao, Y., Chen, S., Lin, J., Bian, J., & Huang, D. (2021). Anti-inflammation activity of flavones and their structure-activity relationship. *Journal of Agricultural and Food Chemistry, 69*(26), 7285–7302. https://doi.org/10.1021/ACS.JAFC.1C02015/SUPPL_FILE/JF1C02015_SI_001.PDF

Wang, Y. C., Chuang, Y. C., & Hsu, H. W. (2008). The flavonoid, carotenoid and pectin content in peels of citrus cultivated in Taiwan. *Food Chemistry, 106*(1), 277–284. https://doi.org/10.1016/J.FOODCHEM.2007.05.086

Wang, D., Zheng, P., & Chen, P. (2019). Production of a recombinant α-l-Rhamnosidase from Aspergillus Niger CCTCC M 2018240 in Pichia pastoris. *Applied Biochemistry and Biotechnology, 189*(3), 1020–1037. https://doi.org/10.1007/S12010-019-03020-2/FIGURES/7

Wu, W., Qiu, X., Ye, X., Zhang, Z., Xu, S., Yao, X., Du, Y., Wu, G., Zhang, R., & Zhu, J. (2025). Naringenin: A potential therapeutic agent for modulating angiogenesis and immune response in hepatocellular carcinoma. *Journal of Pharmaceutical Analysis*. , Article 101254. https://doi.org/10.1016/J.JPHA.2025.101254

Xie, P., jun, H., xin, L., Zhang, C. hong, & Zhang, Y. lei (2015). Phenolic compositions, and antioxidant performance of olive leaf and fruit (Olea europaea L.) extracts and their structure–activity relationships. *Journal of Functional Foods, 16*, 460–471. https://doi.org/10.1016/J.JFF.2015.05.005

Yadav, S., Yadava, S., & Yadav, K. D. S. (2013). Purification and characterization of α-l-rhamnosidase from Penicillium corylopholum MTCC-2011. *Process Biochemistry, 48*(9), 1348–1354. https://doi.org/10.1016/J.PROCBIO.2013.05.001

Yoshinaga, A., Kajiya, N., Oishi, K., Kamada, Y., Ikeda, A., Chigwechokha, P. K., Kibe, T., Kishida, M., Kishida, S., Komatsu, M., & Shiozaki, K. (2016). NEU3 inhibitory effect of naringin suppresses cancer cell growth by attenuation of EGFR signaling through GM3 ganglioside accumulation. *European Journal of Pharmacology, 782*, 21–29. https://doi.org/10.1016/J.EJPHAR.2016.04.035

Yu, C., Li, Q., Tian, J., Zhan, H., Zheng, X., Wang, S., Sun, X., & Sun, X. (2021). A facile preparation of immobilized naringinase on polyethyleneimine-modified Fe 3 O 4 magnetic nanomaterials with high activity. *RSC Advances, 11*(24), 14568–14577. https://doi.org/10.1039/D1RA01449H

Yuan, Y., Shen, J., & Salmon, S. (2023). Developing enzyme immobilization with fibrous membranes: Longevity and characterization considerations. *Membranes, 13*(5), 532. https://doi.org/10.3390/MEMBRANES13050532/S1

Zara, J., Yegres, F., Vargas, N., Morales, S., Cubillan, L., Navas, P., & Márquez-Riquel, M. (2017). Empleo de la Espectroscopia Infrarroja (FT-IR-ATR) como herramienta para la Caracterización del bagazo de caña proveniente de la Sierra Falconiana. *Química Viva, 16*(3), 17–24. https://www.redalyc.org/articulo.oa?id=86354619003.

Zdarta, J., Sałek, K., Kołodziejczak-Radzimska, A., Siwinska-Stefanska, K., Szwarc-Rzepka, K., Norman, M., Klapiszewski, Ł., Bartczak, P., Kaczorek, E., & Jesionowski, T. (2015). Immobilization of Amano Lipase A onto Stöber silica surface: Process characterization and kinetic studies. *Open Chemistry, 13*(1), 138–148. https://doi.org/10.1515/CHEM-2015-0017/MACHINEREADABLECITATION/RIS

Zhang, T., Vavylonis, Di, Durachko, D. M., & Cosgrove, D. J. (2017). Nanoscale movements of cellulose microfibrils in primary cell walls. *Nature Plants, 3*(5), 1–6. https://doi.org/10.1038/nplants.2017.56

Zhang, C., Yang, X., Hu, W., Han, X., Fan, L., & Tao, S. (2020). Preparation and characterization of carboxymethyl chitosan/collagen peptide/oxidized konjac composite hydrogel. *International Journal of Biological Macromolecules, 149*, 31–40. https://doi.org/10.1016/J.IJBIOMAC.2020.01.127

Zhou, W., Zhang, W., & Cai, Y. (2021). Laccase immobilization for water purification: A comprehensive review. *Chemical Engineering Journal, 403*, Article 126272. https://doi.org/10.1016/J.CEJ.2020.126272

Zhu, Y., Jia, H., Xi, M., Li, J., Yang, L., & Li, X. (2017). Characterization of a naringinase from Aspergillus oryzae 11250 and its application in the debitterization of orange juice. *Process Biochemistry, 62*, 114–121. https://doi.org/10.1016/J.PROCBIO.2017.07.012